COST ACTION 18234 TRAINING SCHOOL ON

26-28 July 2022 ▶

COMPUTATIONAL MATERIALS MODELING

For Students & Young Researches
Department of Materials Science and Engineering,
Technion - Israel Institute of Technology

Lectures & practice by:

- **Martijn Marsman**, Department of Physics and Center for Computational Materials Science, University of Vienna, Austria
- **Maytal Caspary Toroker**, Department of Materials Science and Engineering, Technion, Israel
- **Amit Vurgaft**, SKF Company, Israel
- **Jesús Carrete Montaña**, Institute of Materials Chemistry, Technical University of Wien, Austria

Hands-on exercises at the Training School: international participants

	Name	Institute	Country
1	Dr. Mrs. Luiza Epure ?????	Gheorghe Asachi Technical University of Iasi	Romania
2	Dídac-Armand Fenoll	Universitat Autònoma de Barcelona	Spain (Barcelona)
3	Mihai Butolo	University Politehnica of Bucharest	Romania
4	Alexandru Stanciu	University Politehnica of Bucharest	Romania
5	Eleonora Romeo	University of Barcelona	Spain (Barcelona)
6	Miguel Recio Poo	University of Barcelona	Spain (Barcelona)
7	Aniello Langella	University of Naples Federico II, Naples	Italy
8	Mingxue Fu	University of Geneva	Switzerlands
9	Grecenkovs Jurijs	Institute of Solid State Physics, Uniersity of Latvia	Latvia
10	Elina Neilande	Institute of Solid State Physics, Uniersity of Latvia	Latvia
11	Pablo Castro Latorre	University of Barcelona	Spain (Barcelona)
12	Dr. Veerapandian PONNUCHAMY	InnoRenew CoE	Slovenia
13	Emmanouil Pervolarakis	University of Crete	Greece (Crete)
14	Dr. Tijana Djordjević	Vinča Institute of Nuclear Sciences, University of Belgrade	Serbia
15	Rafaela Giappa	University of Crete	Greece (Crete)
16	Vasil Ivanov	Sofia University	Bulgaria
17	Dr. Vipin Kumar	Tel Aviv Univeristy	Israel
18	Radhey Yadav	Ariel University	Israel

Program for the training school

Includes lectures (auditorium), tutorials (computer room), visitor center tour and dinner.

https://mats.net.technion.ac.il/

Access to internet: Click on **TechPublic** in the network options (no password required).

Charge Transport Calculations Across Materials

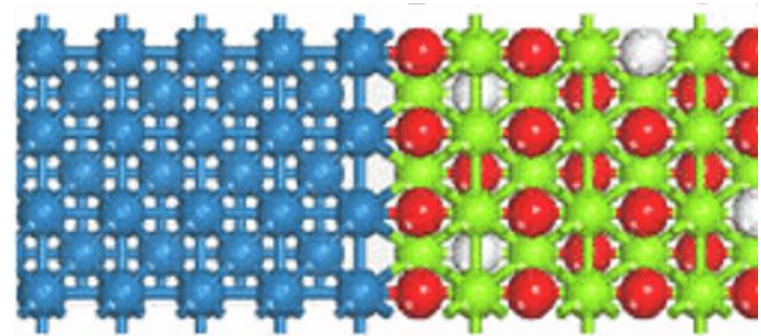Maytal Caspary Toroker

Department of Materials Science and Engineering,
Technion – Israel Institute of Technology

Outline # 1

- Motivation for studying material interfaces
- Novel algorithm for charge transport calculations for materials: applications and case studies.
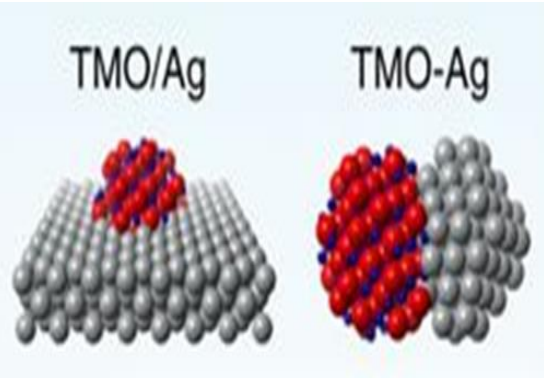

Material interface

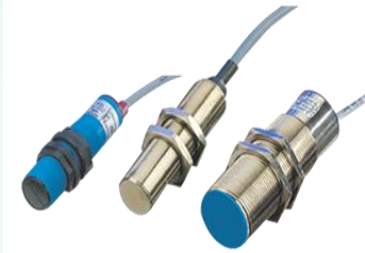# Material Surfaces and Interfaces Play a Key Role in Several Fields

Appliances

Ships

Catalysis

Sensors

Electrochemical Devices

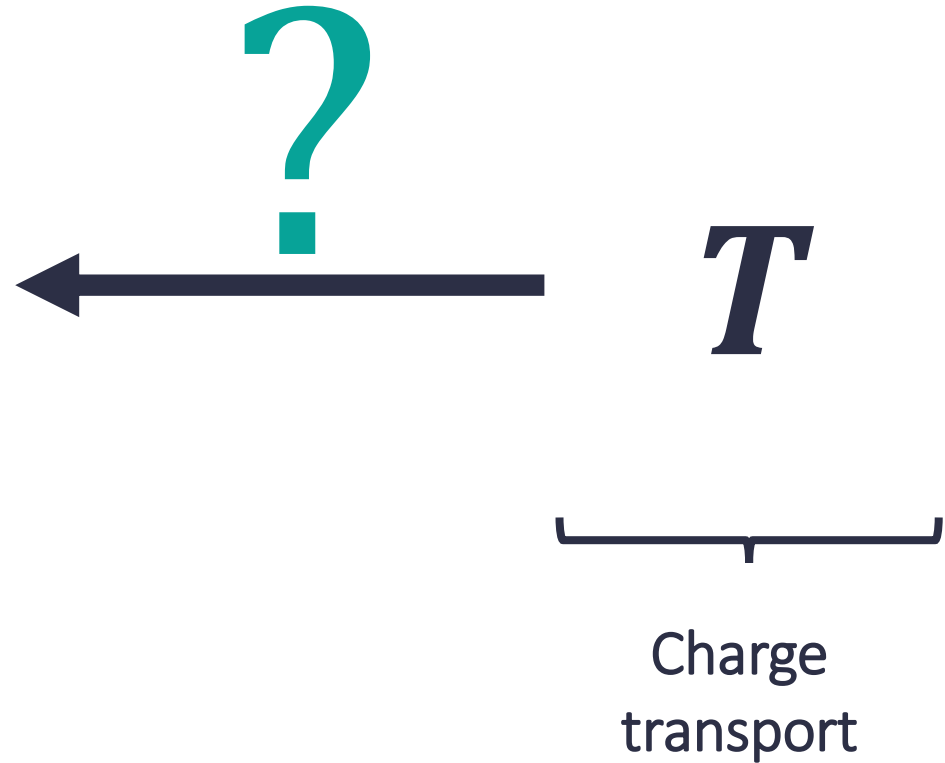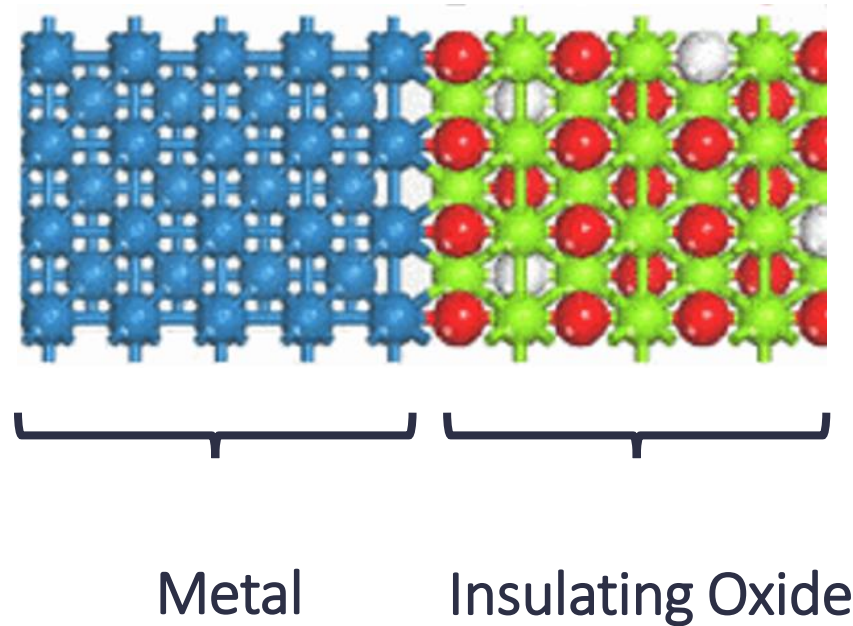Turbine Blades

Asteroids

Minerals

Transistors

Batteries

Existing Methodologies are Limited in their Ability to Provide Structure-Function Fundamental Understanding

Metal   Insulating Oxide

T

Charge transport

Applications and case studies:

- Dielectrics for transistors.

  L. Teitz and M. Caspary Toroker, Adv. Func. Mat., 1808544 (2019).

- Semiconductors for transistors.

  G. Ben-Melech Stan and M. Caspary Toroker, Molecular Physics 119, 15 (2019).

  G. Ben-Melech Stan, K. Dhaka, M. Caspary Toroker, Isr. J. Chem. 60 (8-9), 888 (2020).

- Quantum computing junctions.

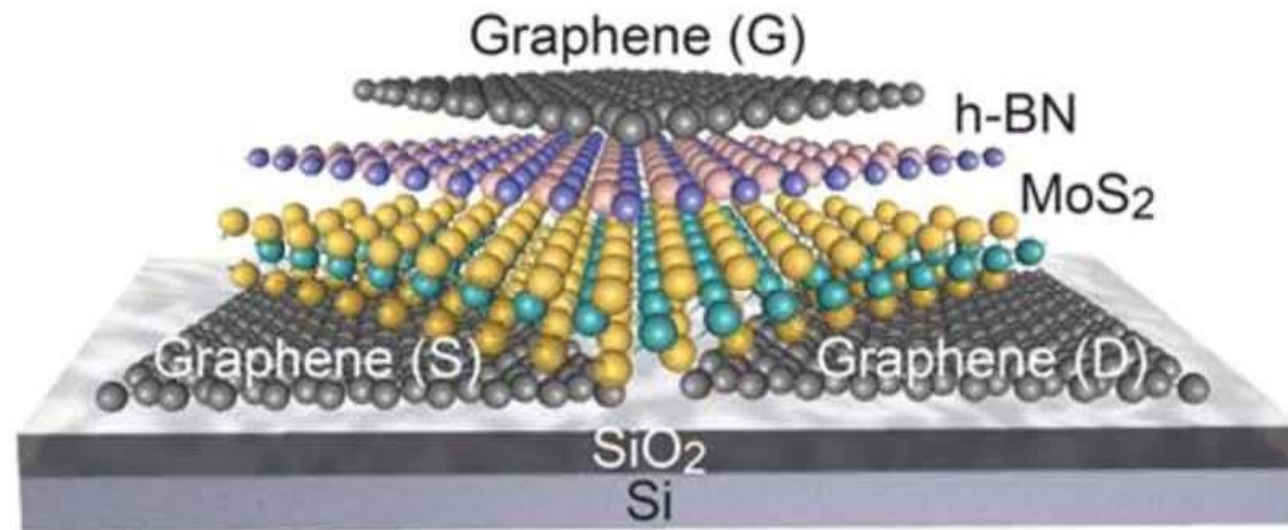 A. Reshef and M. Caspary Toroker, NPJ Computational Materials 7, 1 (2021).

- Electrodes in electrochemistry.

  O. Neufeld and M. Caspary Toroker, J. Chem. Theo. Comp. 12, 1572 (2016).

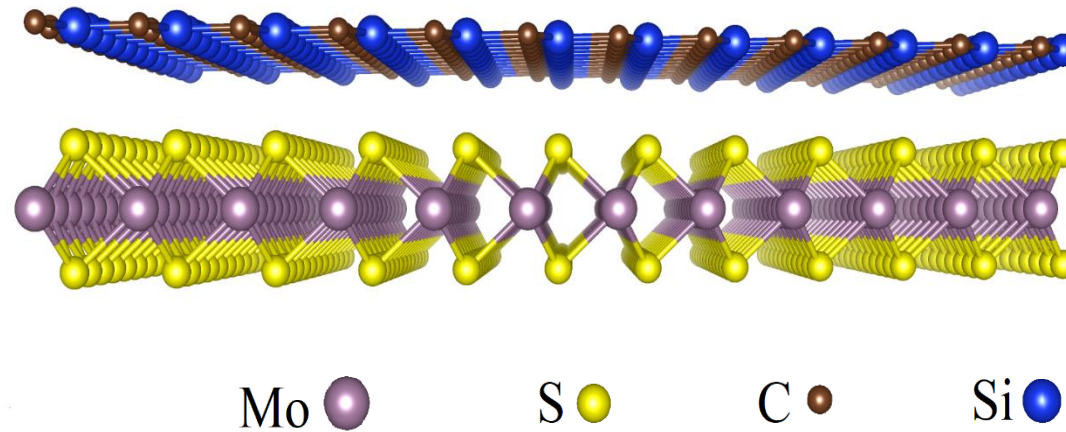 Y. Tovi and M. Caspary Toroker, J. Chem. Phys. 153, 024104 (2020).

The role of charge transport in devices

In dielectric materials, charge should not leak to the gate electrode.
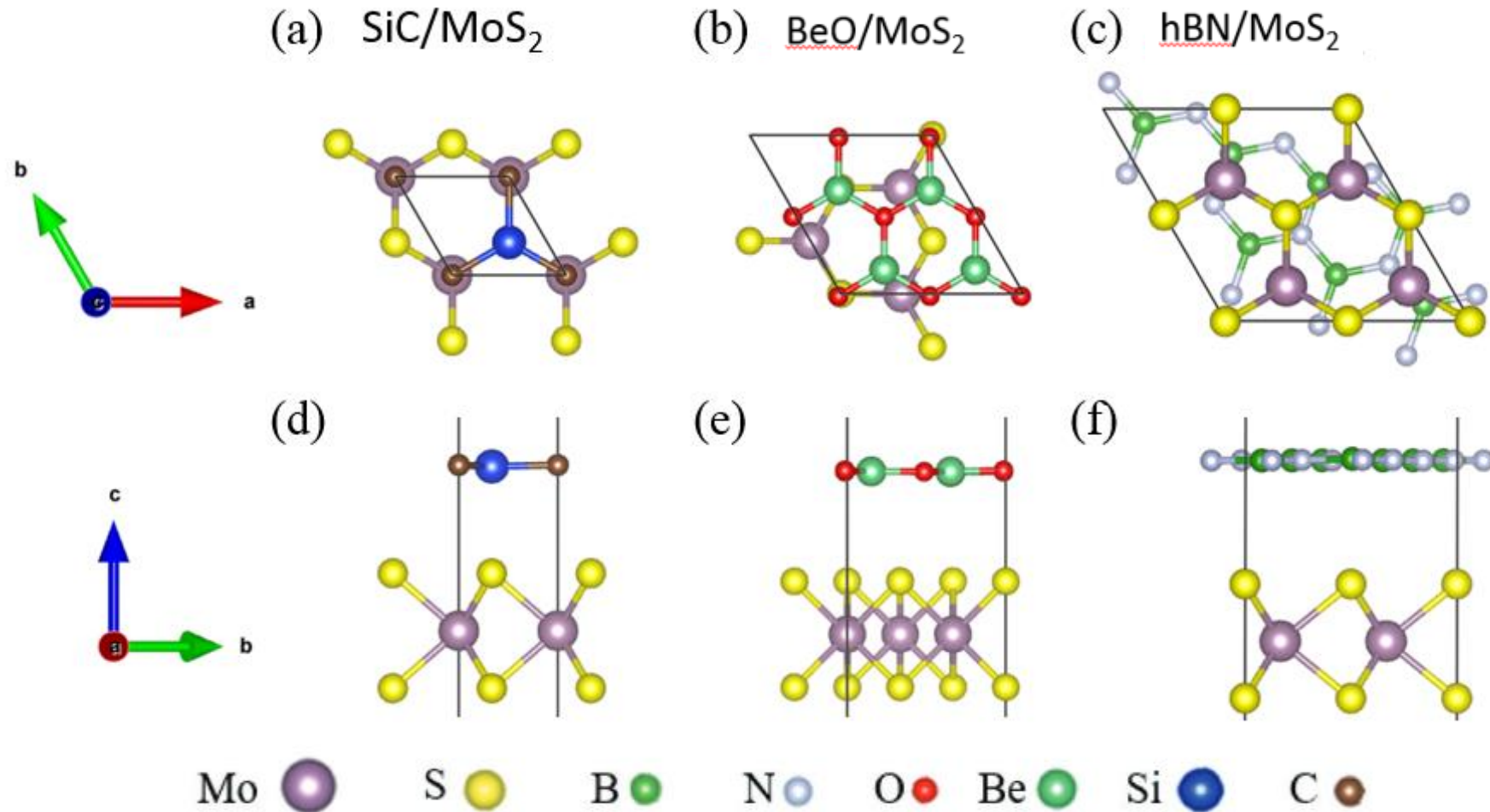

T. Roy, M. Tosun, J. S. Kang, A. B. Sachid, S. B. Desai, M. Hettick, C. C. Hu, A. Javey, *ACS Nano* 2014, 8, 6, 6259–6264

Atomic model for the MoS$_2$/SiC interface:

Mo ⬤ S ⬤ C ⬤ Si ⬤

L. Teitz and M. Caspary Toroker, Adv. Func. Mat., 1808544 (2019).

Applications: Dielectric materials

(a) SiC/MoS$_2$ (b) BeO/MoS$_2$ (c) hBN/MoS$_2$

(d) (e) (f)

Mo S B N O Be Si C

L. Teitz and M. Caspary Toroker, Adv. Func. Mat., 1808544 (2019).

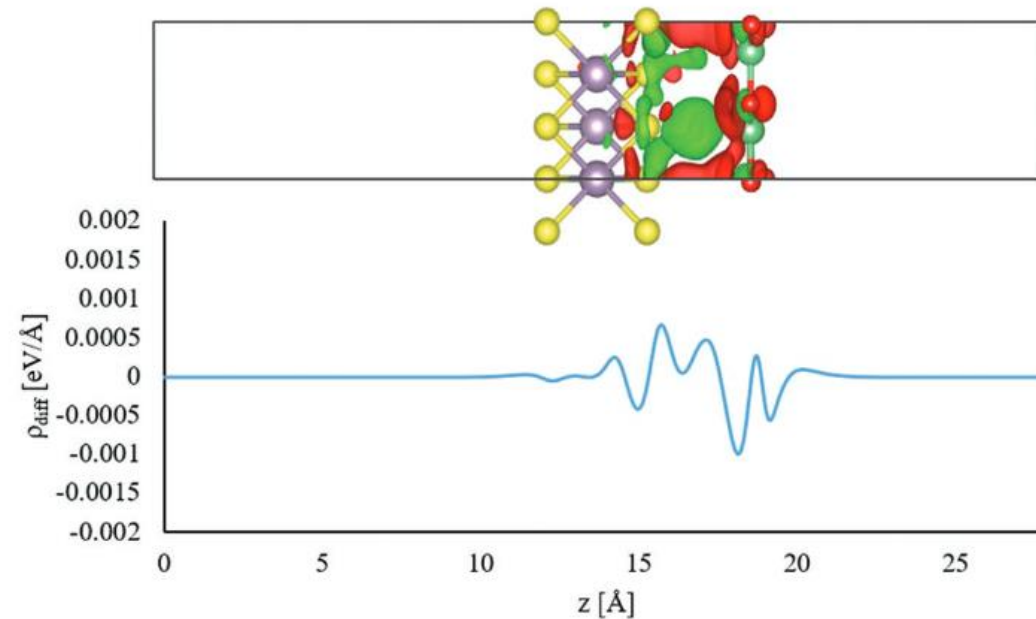# Dielectric materials: small charge density change

Table 1. Bond lengths of the isolated monolayer materials and of the materials at the interface, Bader charge redistribution at the interface, adhesion energies, and physical separation at each interface.

Interface	d [Å]	ε_0	E_{adh}[meV/Å^2]	Charge transfer [e]	Mo-S bond length [Å]		Material bond length [Å]	
					At interface	Isolated	At interface	Isolated
BeO/MoS$_2$	3.31	2.91	−5.65	0.00175	2.40	2.41	1.57	1.55
SiC/MoS$_2$	2.94	3.21	−47.37	0.0333	2.40	2.41	1.81	1.79
hBN/MoS$_2$	3.29	3.00	−8.02	0.0232	2.44	2.41	1.43	1.45

L. Teitz and M. Caspary Toroker, Adv. Func. Mat., 1808544 (2019).

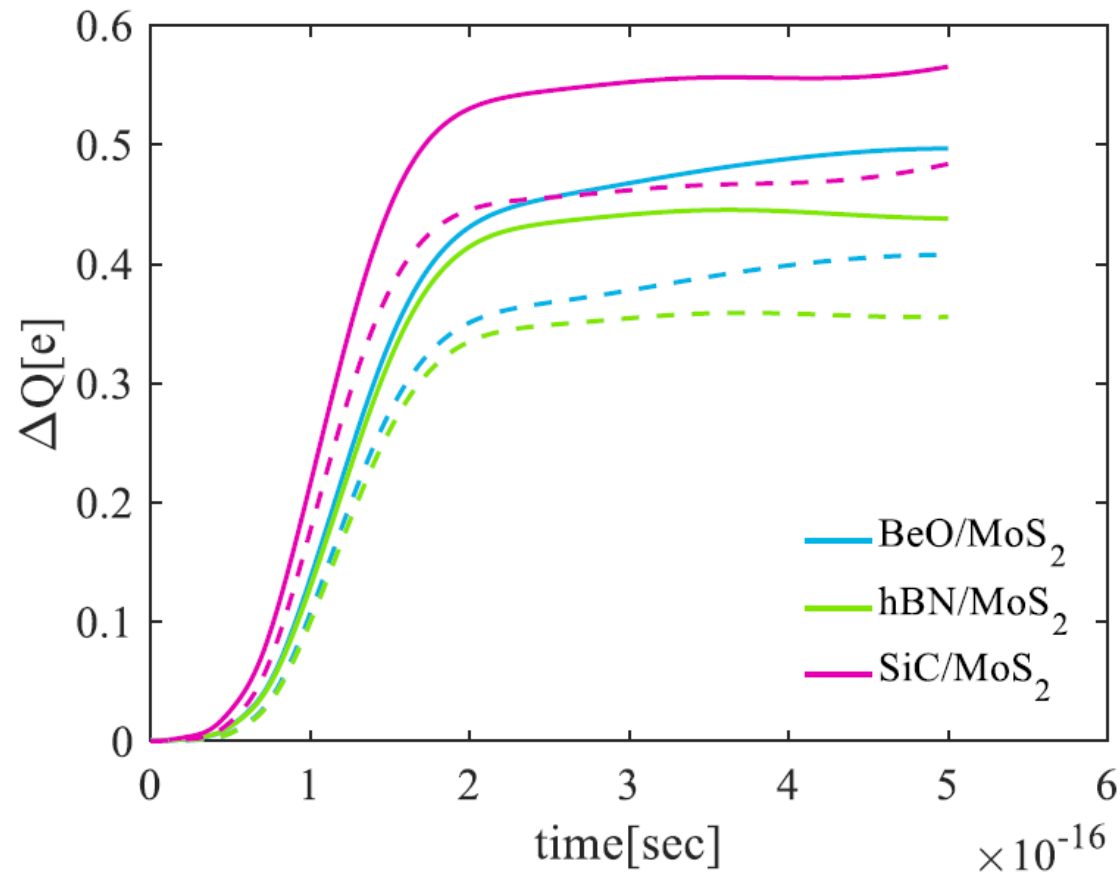# Comparing charge transport between dielectric materials: correlation to potential energy heights

Table 3. Calculated tunnel barrier heights (Φ_{TB}) and transmission coefficients (Θ) of each interface, for initial energies equal to the CBM or VBM.

Interface	Φ_{TB} [eV]	Θ	
		VBM	CBM
BeO/MoS$_2$	18.68	0.40	0.49
SiC/MoS$_2$	16.17	0.47	0.56
hBN/MoS$_2$	25.05	0.36	0.44

L. Teitz and M. Caspary Toroker, Adv. Func. Mat., 1808544 (2019).

Potential energy of a dielectric material

A large height at the MoS2/SiC interface:
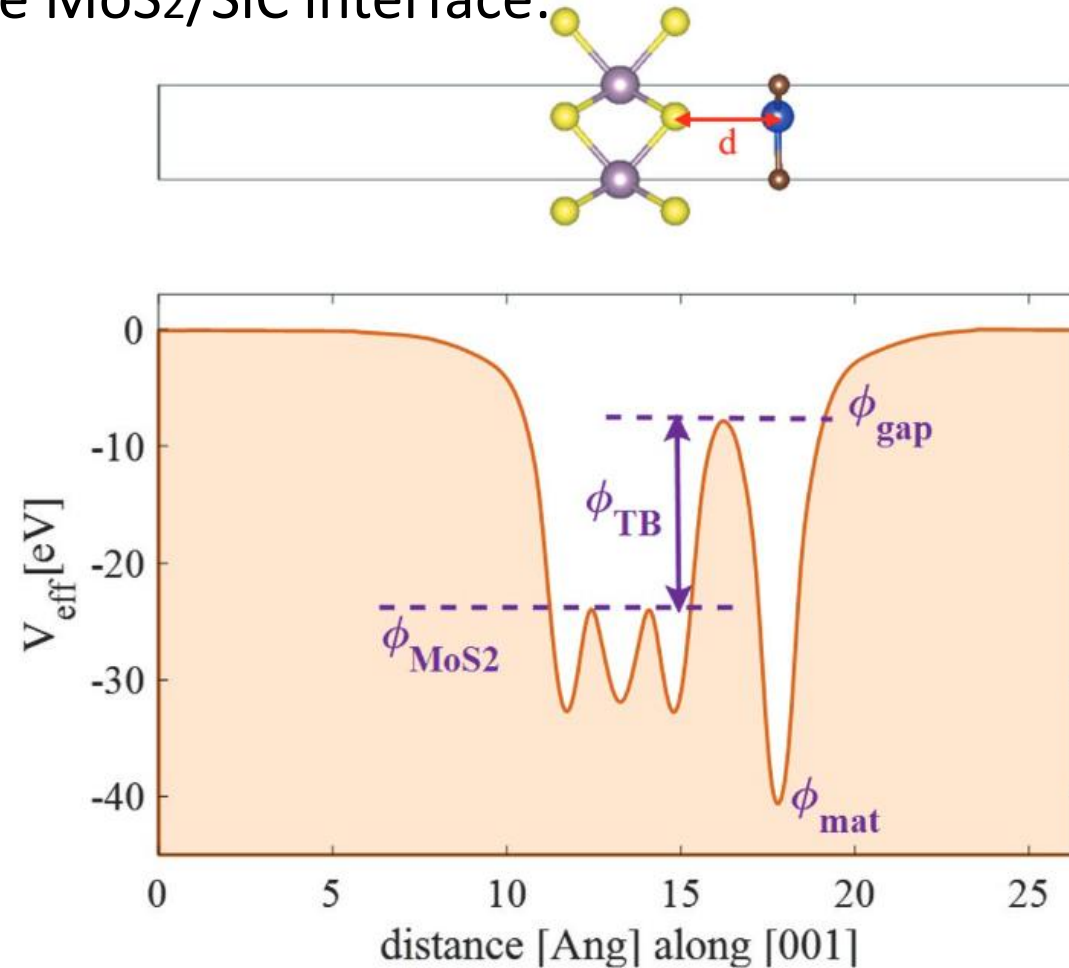
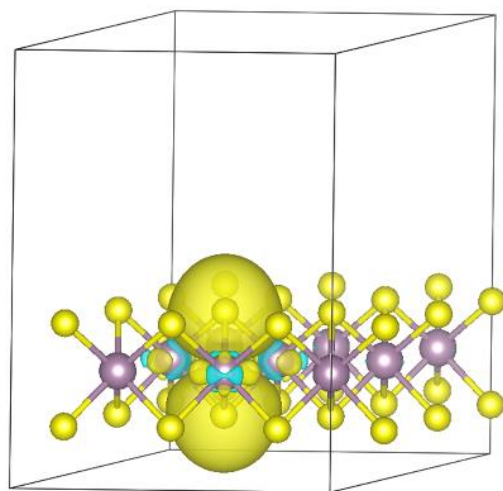L. Teitz and M. Caspary Toroker, Adv. Func. Mat., 1808544 (2019).

Take a look at the dynamics in a dielectric:

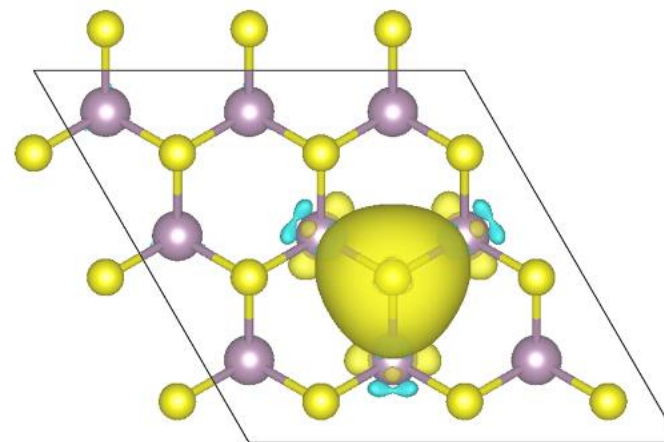Some charge escapes through the MoS$_2$/BeO interface:

L. Teitz and M. Caspary Toroker, Adv. Func. Mat., 1808544 (2019).
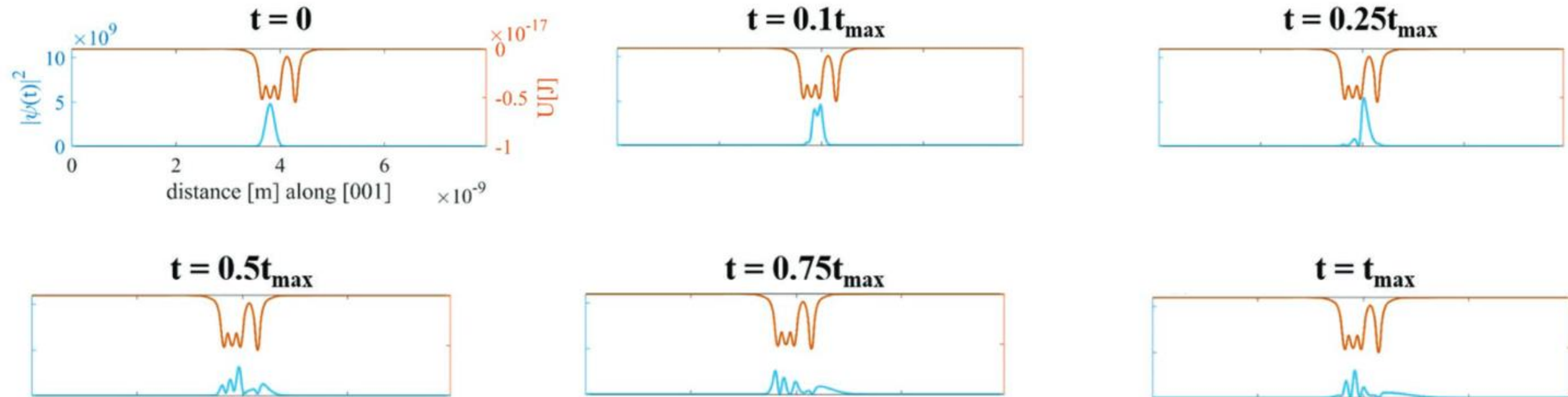
Quantum dynamics near defects in the semiconductor MoS₂

Charge density of MoS2 monolayer with a
sulfur vacancy of type 11% V-2S.

Isometric view   top view

● Mo
● S

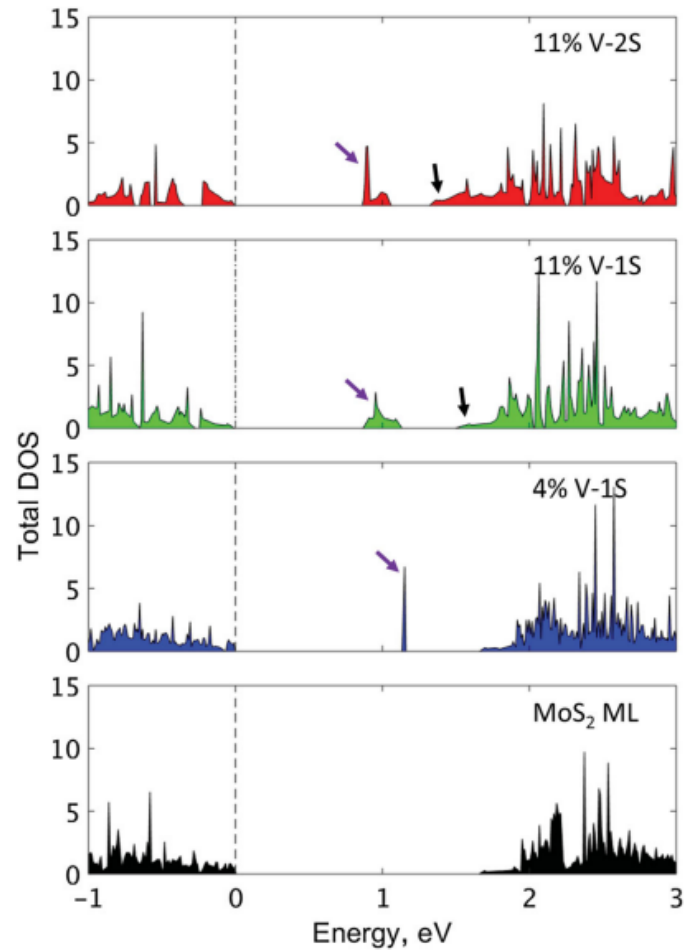G. Ben-Melech Stan and M. Caspary Toroker, Molecular Physics 119, 15 (2019).

Figure 2. Total density of states for MoS$_2$ monolayer without and with S vacancy. The purple arrow points to the mid-gap states seen for all ML with S vacancy defects, and the black arrow points to conduction band edge states, mostly seen for ML with 11% V-1S

Vacancy-induced charge is located on Mo 1st neighbors:

G. Ben-Melech Stan and M. Caspary Toroker, Molecular Physics 119, 15 (2019).
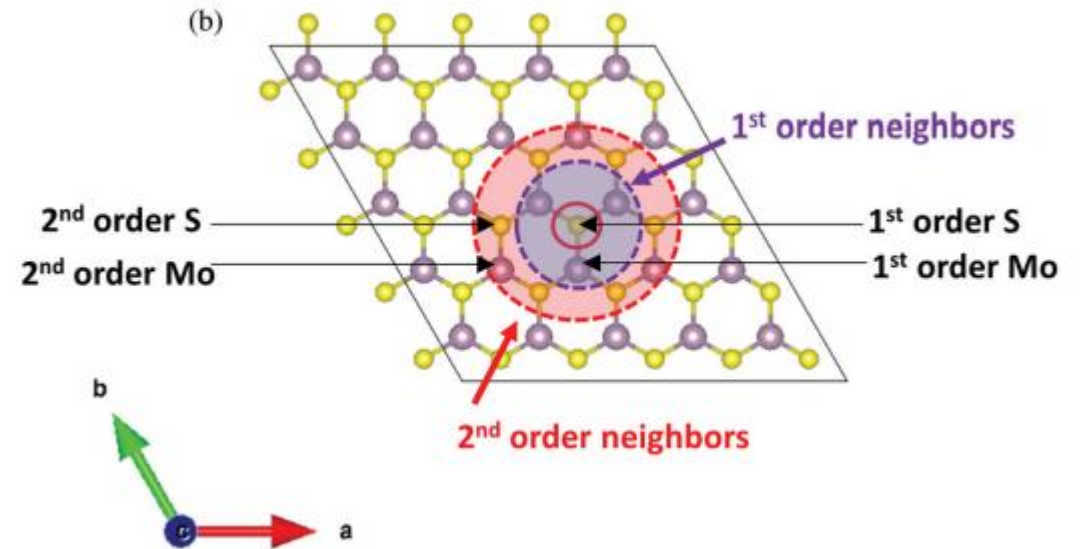
Quantum dynamics near defects in MoS₂

A larger transport without vacancies:

G. Ben-Melech Stan and M. Caspary Toroker, Molecular Physics 119, 15 (2019).
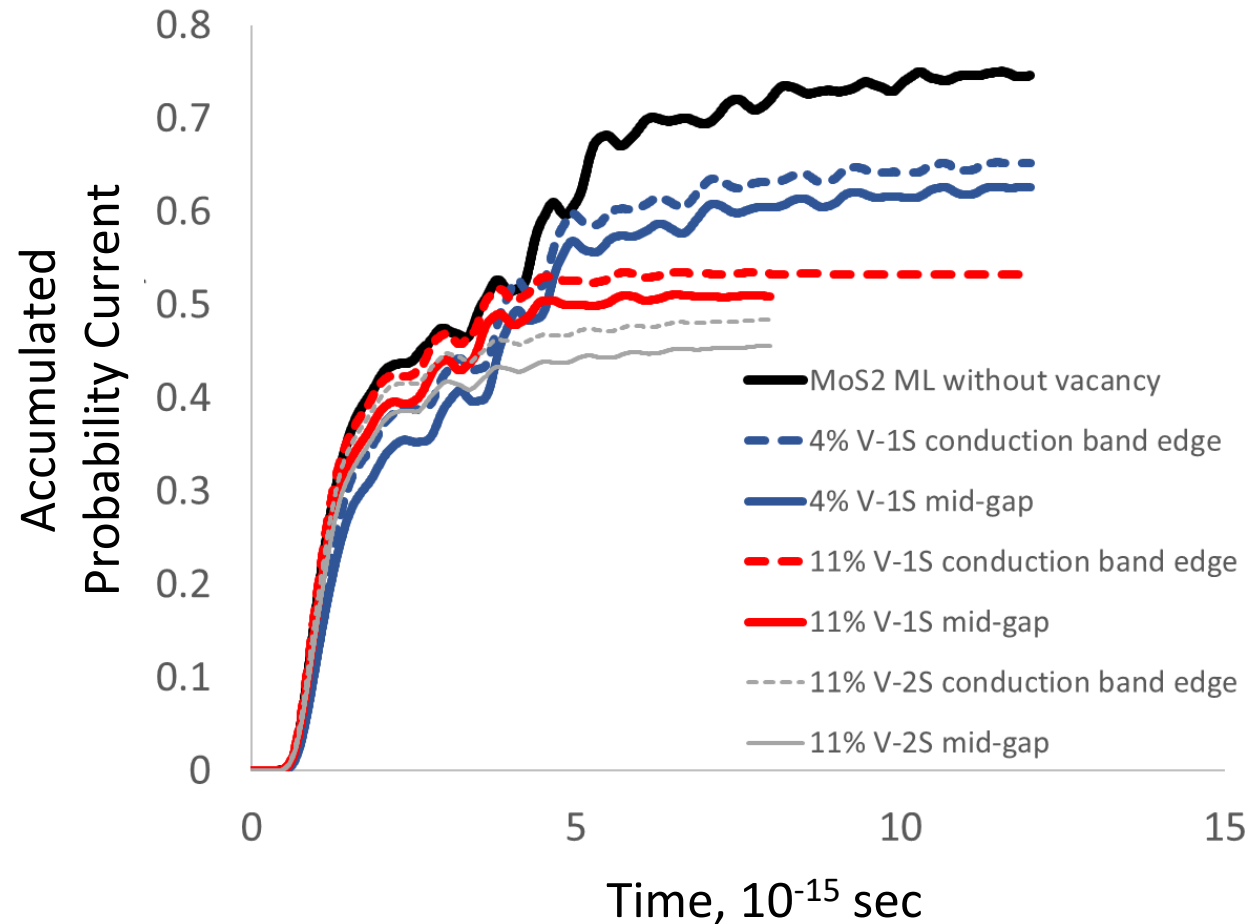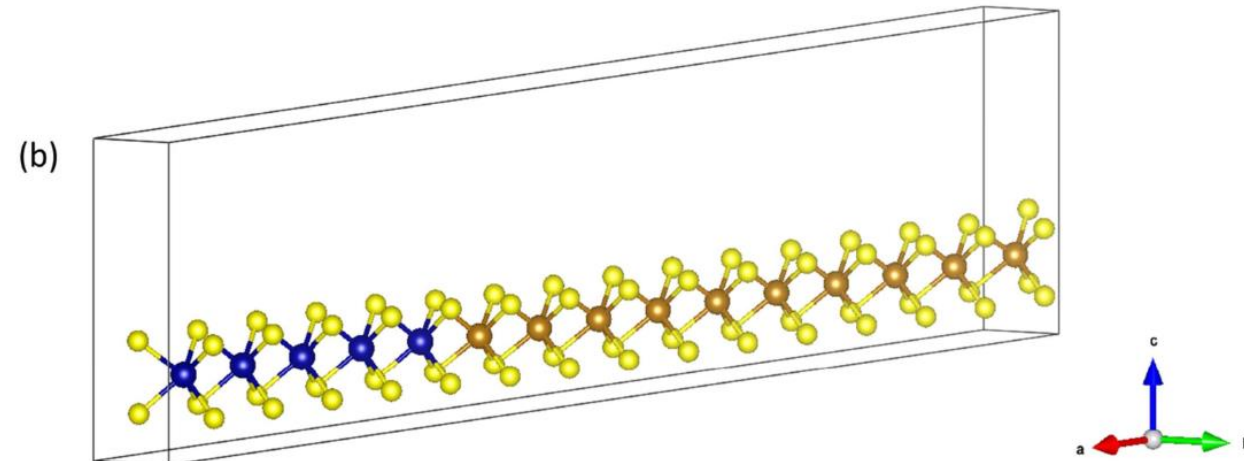
Metal/Semiconductor interfaces: replacing the metal

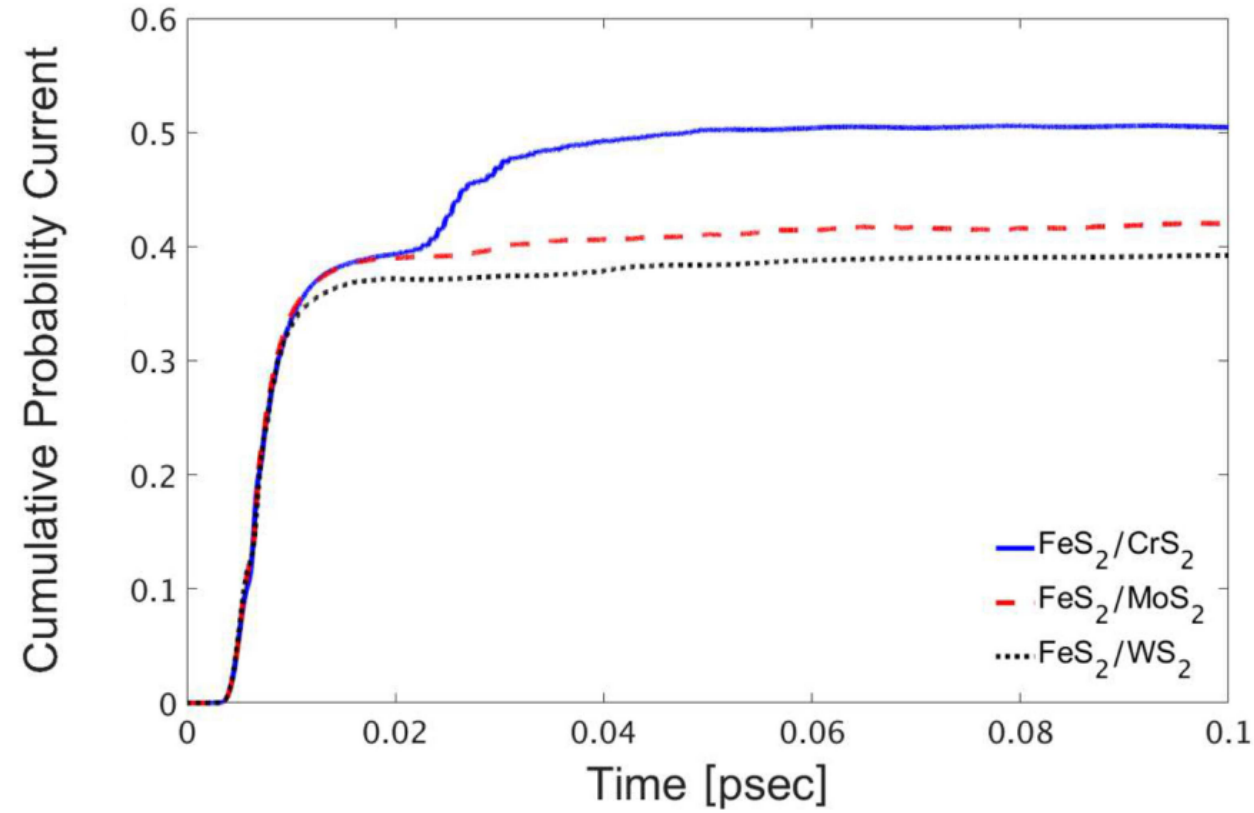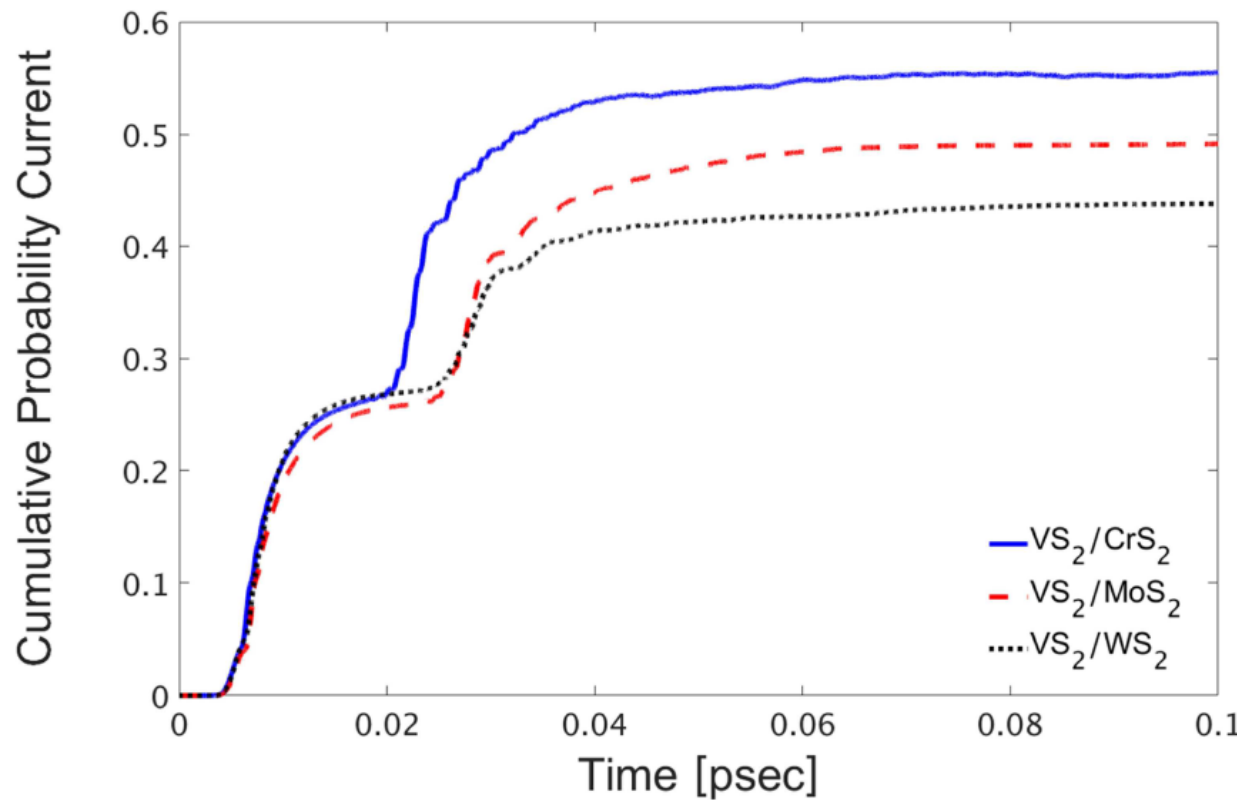Selection of different metals of the atomic interface model:

Table 1. Calculated characteristics of metal/semiconductor/metal systems.

Metal/ semiconductor	Metal length [Å]	Semiconductor length [Å]	Lattice Mismatch [%][23]
FeS_2/CrS_2	31.45	14.99	2.9
FeS_2/MoS_2	32.06	15.41	1.5
FeS_2/WS_2	32.02	15.43	1.2
VS_2/CrS_2	31.59	15.05	4.2
VS_2/MoS_2	32.26	15.42	3.2
VS_2/WS_2	32.42	15.54	0.1

(b)

G. Ben-Melech Stan, K. Dhaka, M. Caspary Toroker, Isr. J. Chem. 60 (8-9), 888 (2020).

VS$_2$/CrS$_2$ have the highest current:

G. Ben-Melech Stan, K. Dhaka, M. Caspary Toroker, Isr. J. Chem. 60 (8-9), 888 (2020).

The role of charge transport in catalysis

Particularly in the area of catalysis, charge needs to transport to the surface for redox reactions.

$$H_2O_{(l)} \rightarrow H_{2(g)} + \frac{1}{2}O_{2(g)}$$
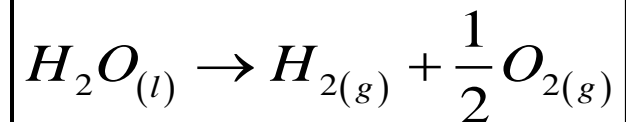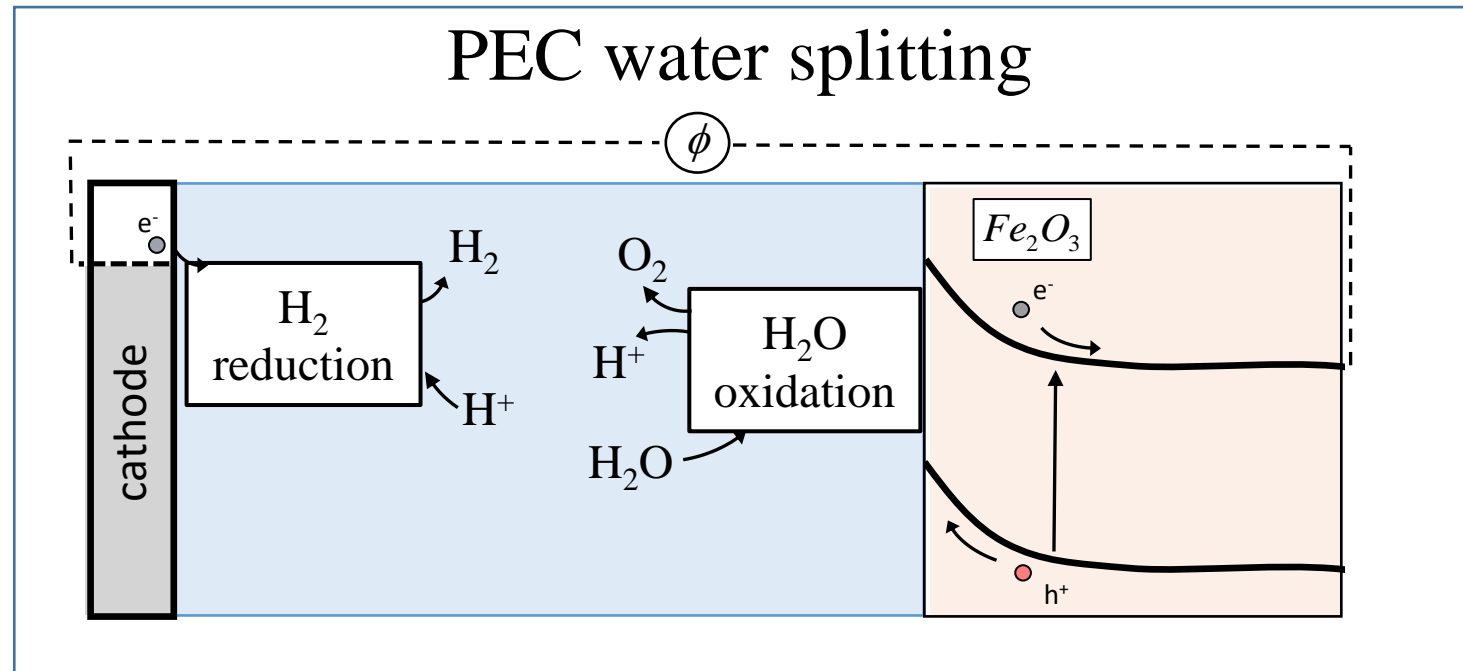
Several back contacts for Fe$_2$O$_3$
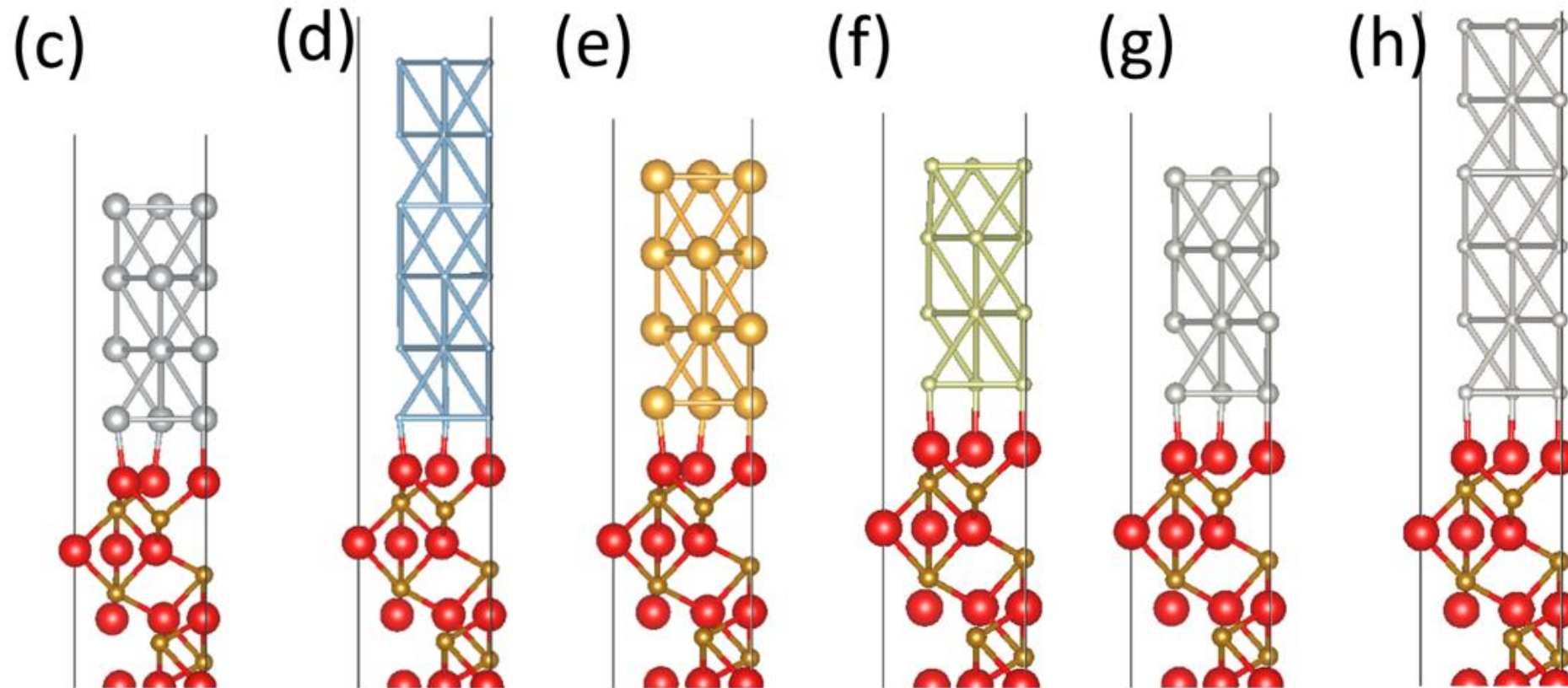
The method offers to screen different materials:

Figure 2. (a) Fe$_2$O$_3$ (0001) oxygen-terminated slab. (b) FCC metal (111) slab. Blue shading represents the unit cell of the metal and Fe$_2$O$_3$ which creates the interfaces. (c)-(h) Relaxed Fe$_2$O$_3$/Mt interfaces for Mt = Ag, Al, Au, Ir, Pd, and Pt, respectively. Created using VESTA.[90]

O. Neufeld and M. Caspary Toroker, J. Chem. Theo. Comp. 12, 1572 (2016).

Comparing between metals
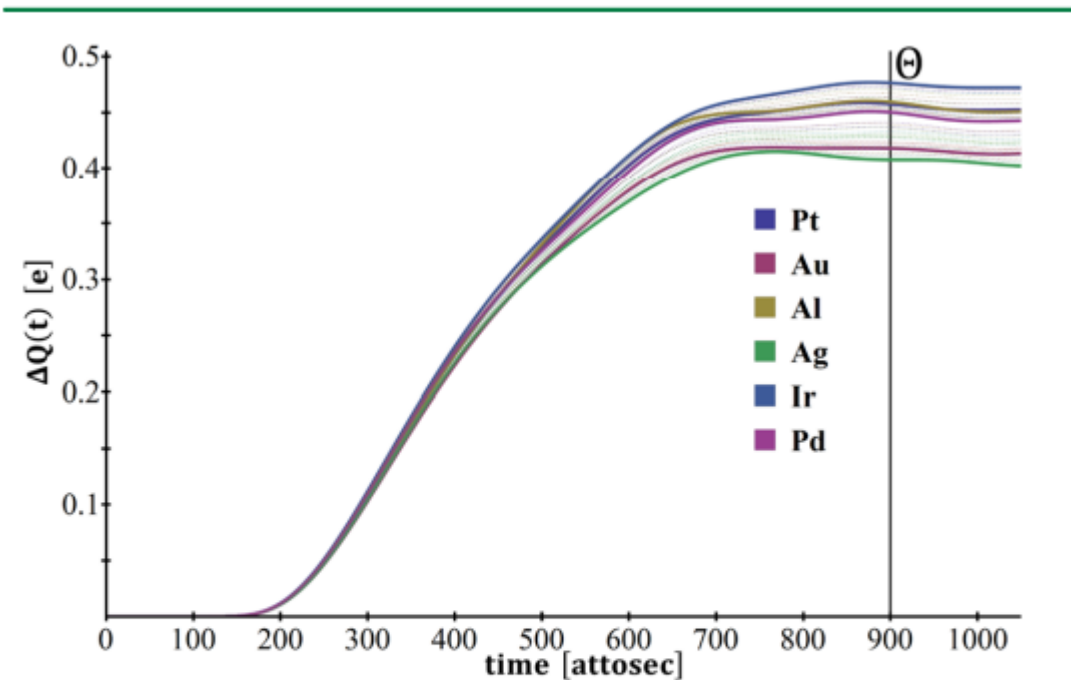
Ir metal shows best performance, Ag the least:

Figure 8. Computed transport probability $\Delta Q(t)$ for all Fe_2O_3/Mt interfaces. Solid plots represent pure metals for which a DFT calculation was performed as denoted in the legends; dashed lines represent alloys which were fast screened without the DFT calculation.

O. Neufeld and M. Caspary Toroker, J. Chem. Theo. Comp. 12, 1572 (2016).

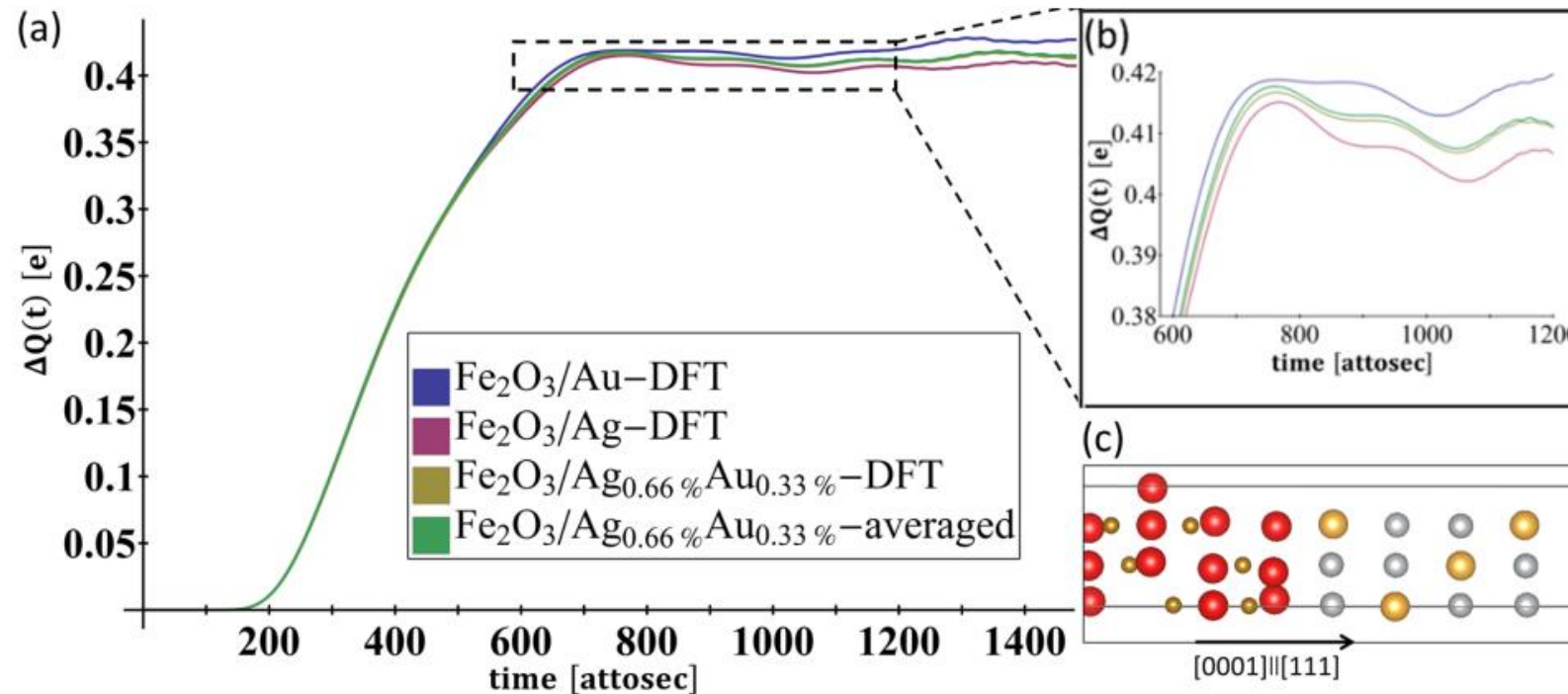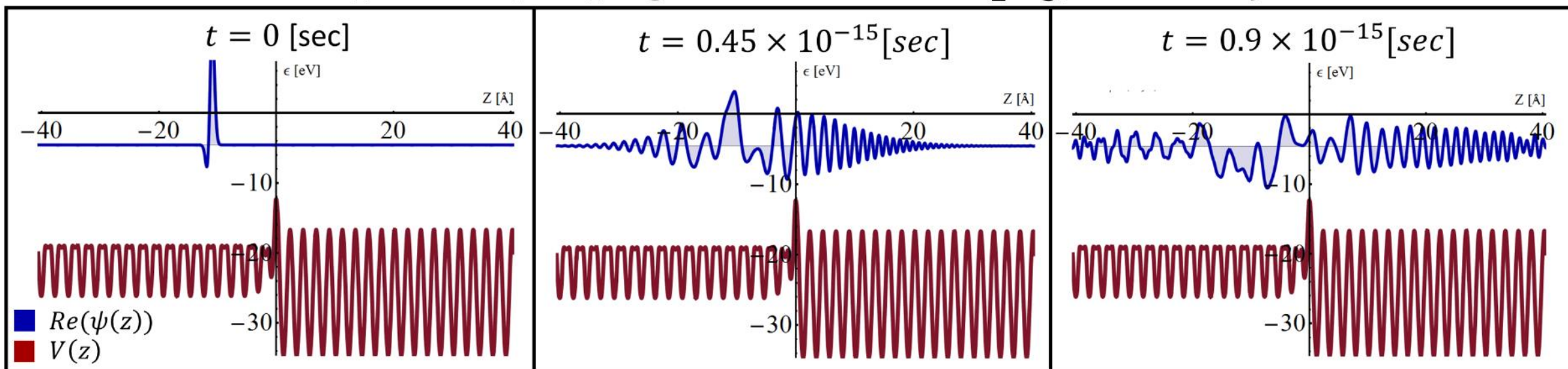# Prediction of transmission through a Ag/Au alloy

The method can be used for alloys:

Figure 4. (a) Electron transport probability, $\Delta Q(t)$, for the alloy system, with $Fe_2O_3/Ag_{0.66}Au_{0.33}$ from DFT, and from an analytically averaged potential energy. (b) Magnification of (a) around the plateau (at area marked with dashed lines). (c) The relaxed DFT structure at Ag66% at., Au33% at., with an even spread of atoms. Atom colors red, gold, yellow, and silver represent oxygen, iron, gold, and silver atoms, respectively.
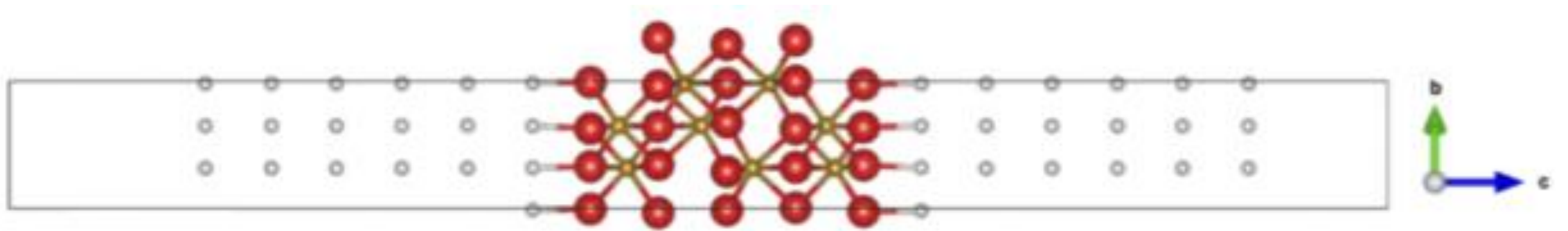
O. Neufeld and M. Caspary Toroker, J. Chem. Theo. Comp. 12, 1572 (2016).

Wavepacket propagation in the Fe_2O_3/Pt interface

O. Neufeld and M. Caspary Toroker, J. Chem. Theo. Comp. 12, 1572 (2016).

The main coordinate is in the normal to the interface, the transport direction (z).

$$V(z) = \iint V(x,y,z)\,dx\,dy$$

$$V(x,z) = \int V(x,y,z)\,dy$$

X

Z

Y. Tovi and M. Caspary Toroker, J. Chem. Phys. 153, 024104 (2020).

Additional lowest energy pathways through crystallographic available directions.

FIG. 6. Snapshots from the time evolution of $|\Psi|^2$ in the Pt/Fe$_2$O$_3$ interface. All images are close-ups of the interface area. Color bar units are given in Å^{-2}.
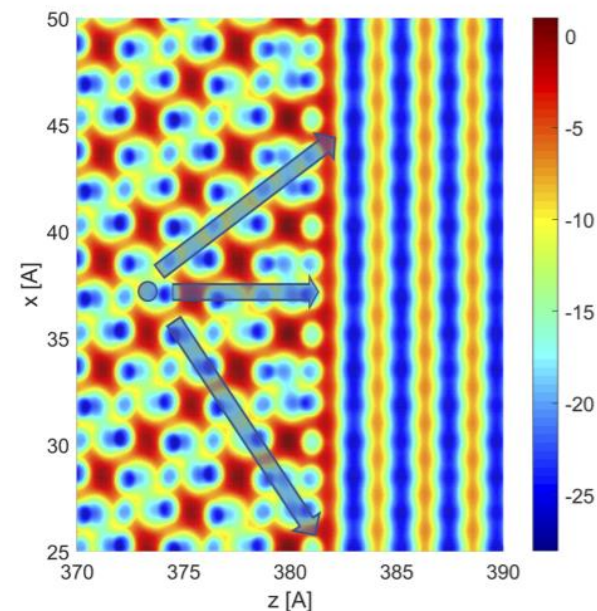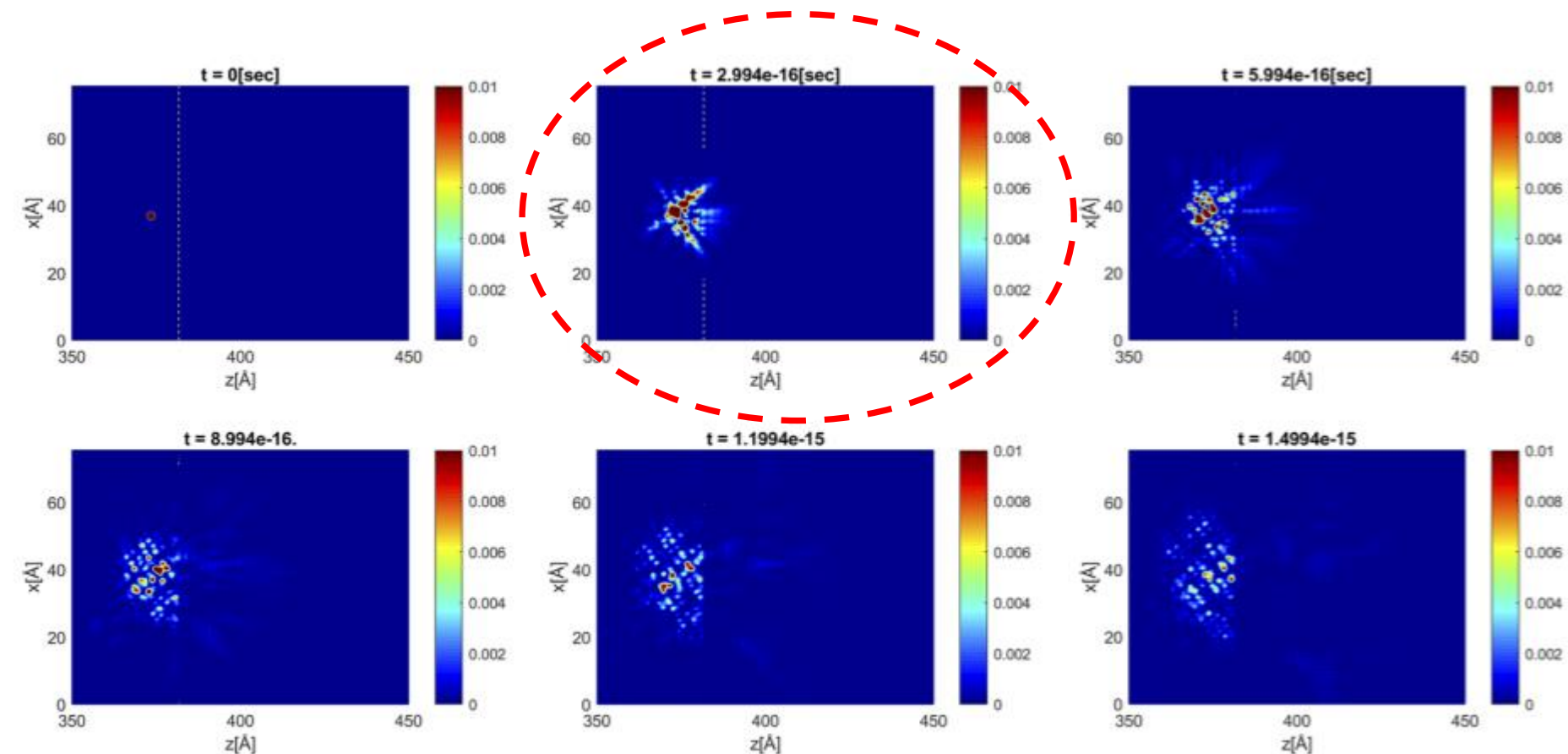
FIG. 10. Proposed dominant paths for the wave function in the Pt/Ox interface. The preferred paths are marked by arrows, and the center of the initial Gaussian is marked by a circle.

Y. Tovi and M. Caspary Toroker, J. Chem. Phys. 153, 024104 (2020).

The 1D model is valuable for qualitative comparisons between materials.
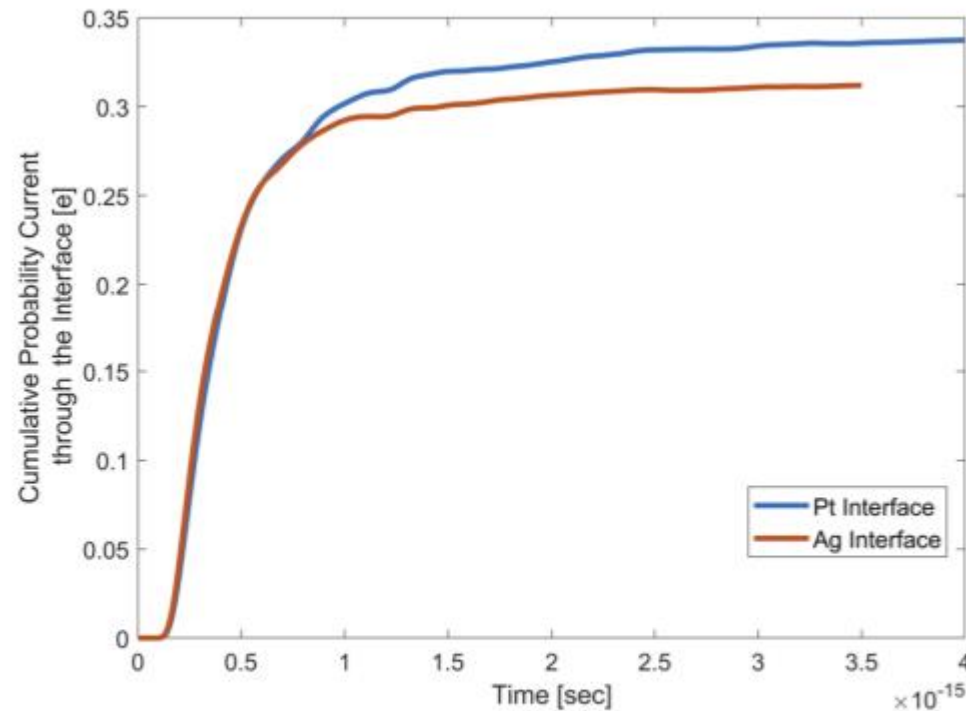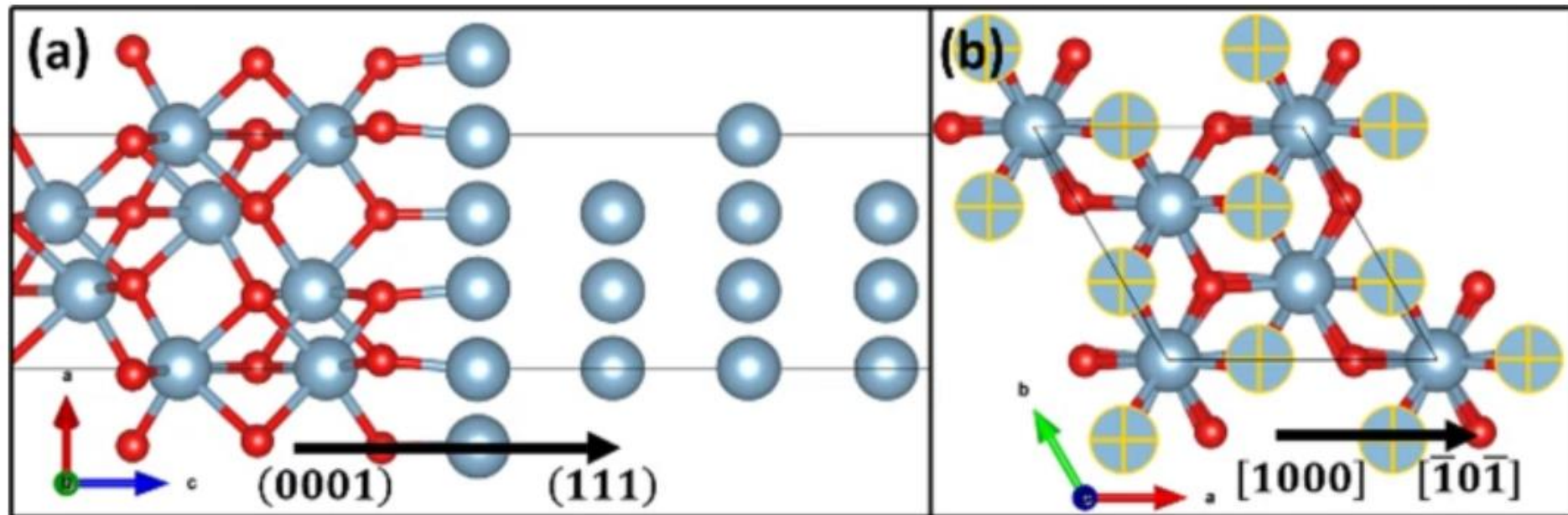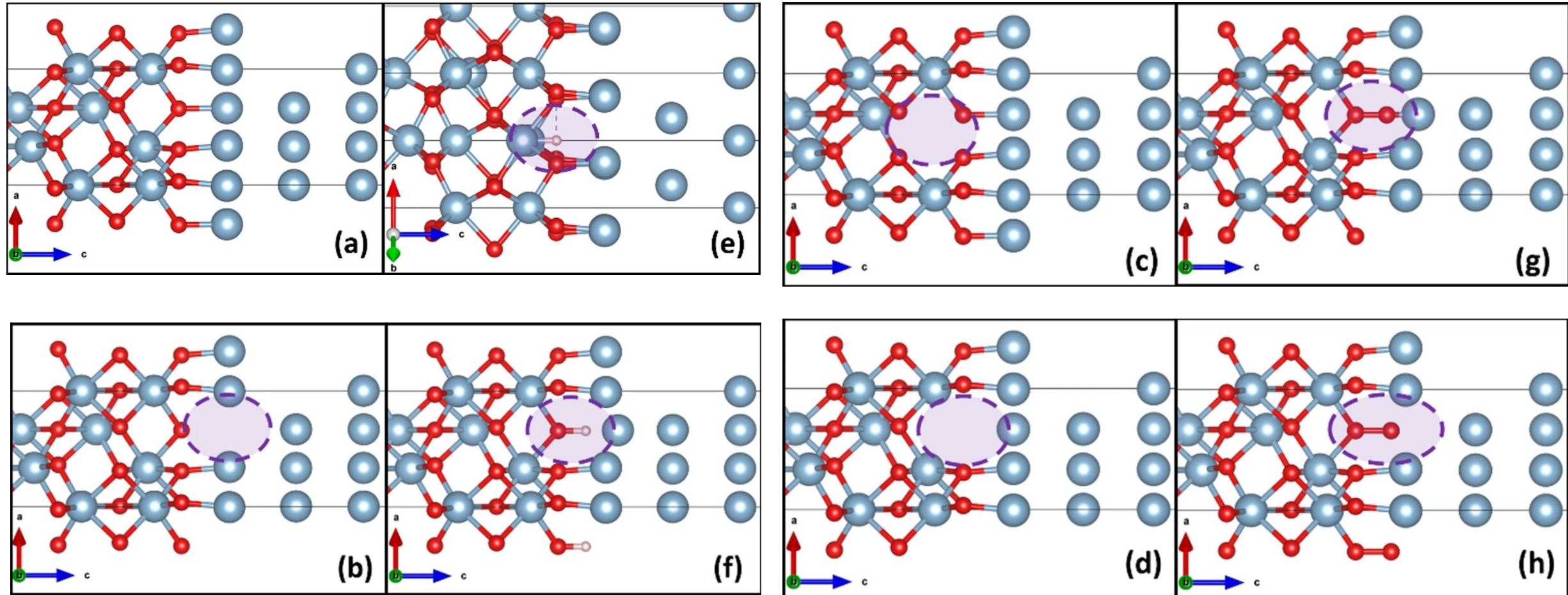

FIG. 5. Time-cumulative, x-integrated, z-directed current through the metal/Fe2O3 interface. The value at the plateau is the transmission.

Y. Tovi and M. Caspary Toroker, J. Chem. Phys. 153, 024104 (2020).

Al/Al2O3 interfaces used for qubits:

A. Reshef and M. Caspary Toroker, NPJ Computational Materials 7, 1 (2021).

a Reference structure. b Al vacancy in the metal cap. c Al vacancy in the oxide. d O vacancy in the oxide, e trapped H, f trapped OH, g trapped O_2, and h Al for O substitution.

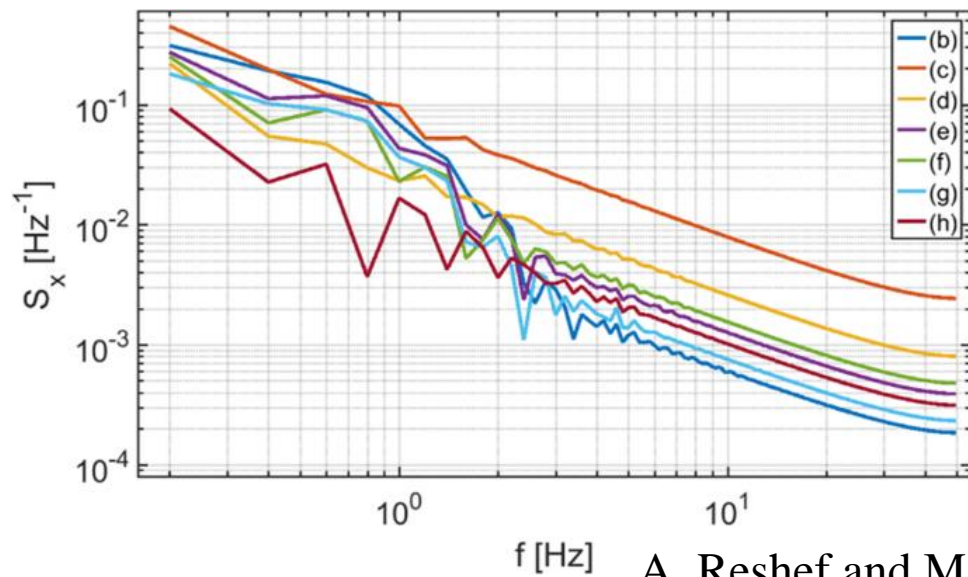A. Reshef and M. Caspary Toroker, NPJ Computational Materials 7, 1 (2021).

Wave packet propagation:
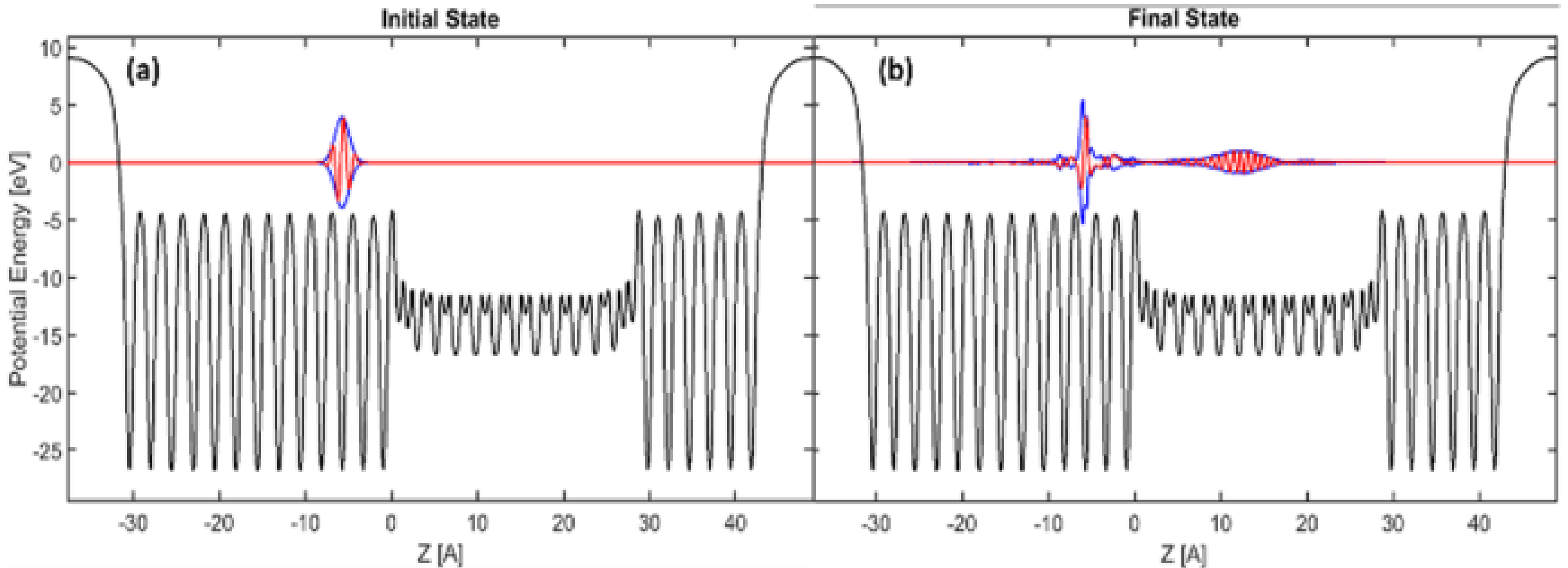
A. Reshef and M. Caspary Toroker, NPJ Computational Materials 7, 1 (2021).

Comparing to experimental noise signature

Model	B fit	Deviation (%)	R^2
(b)	1.213	21.27	0.958
(c)	0.902	−9.79	0.972
(d)	0.908	−9.22	0.939
(e)	1.054	5.39	0.987
(f)	0.990	−1.03	0.989
(g)	1.086	8.56	0.902
(h)	0.911	−8.85	0.926

Power spectral density: $S_x(f) \propto f^{-\beta}.$

The presence of OH molecule, in interstitial sites in the vicinity of the interface, generate noise with Fourier component with very good match to the characteristic shape of flicker noise.

A. Reshef and M. Caspary Toroker, NPJ Computational Materials 7, 1 (2021).

Summary of outline #1:

- The algorithm was tested on a variety of **systems and applications**.
- The approach enable to **view/simulate the electron** and calculate probability for charge transfer.
- The method enables to **design new materials** by correlating functionality to intrinsic kinetic barrier heights.

Outline # 2

- Structure of **potential energy of materials**
- **Initial condition/location** of the electron
- The solution: **time propagation**
- How to calculate electronic current? **Flux as an observable**

Time Dependent Schrödinger Equation for calculating charge transport through materials

The time dependent Schrödinger equation is:

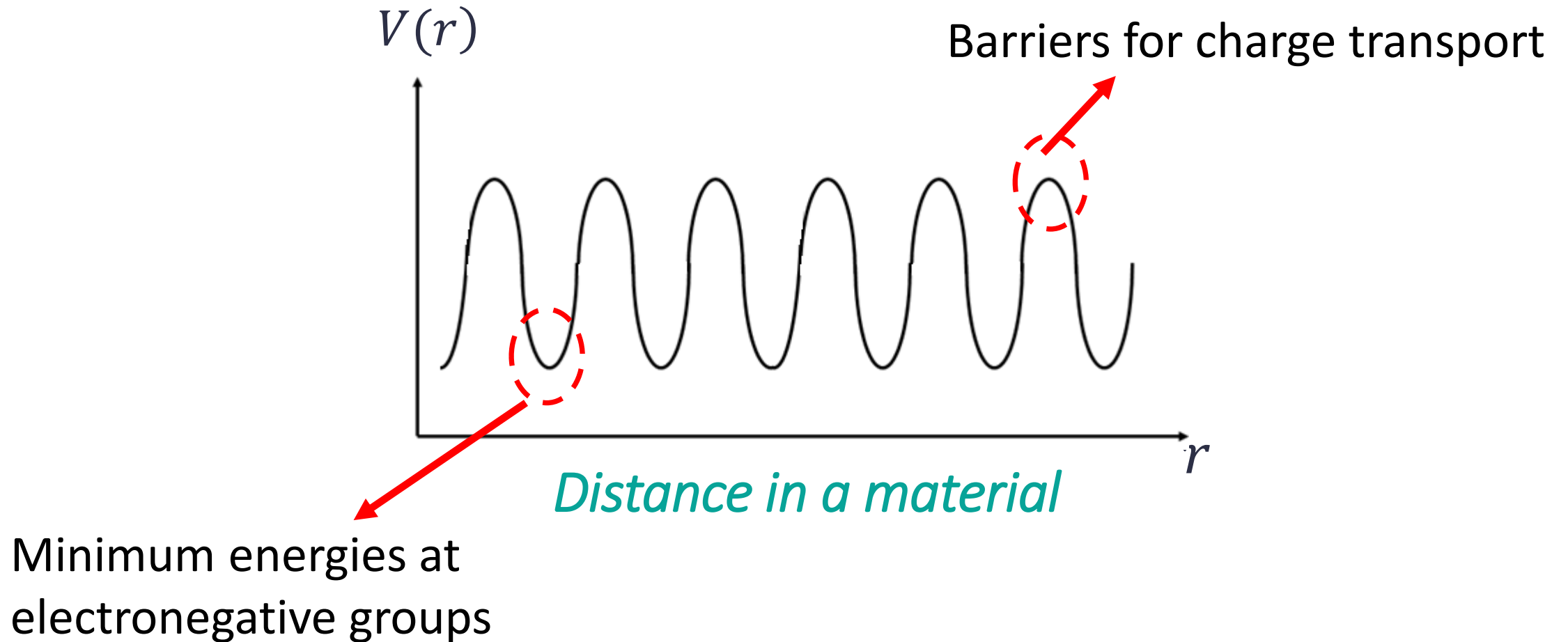$$i\hbar \frac{\partial}{\partial t}|\psi(t)\rangle = \widehat{H}|\psi(t)\rangle$$

The Hamiltonian includes kinetic and potential energies:

$$\widehat{H} = \widehat{T} + \widehat{V}$$
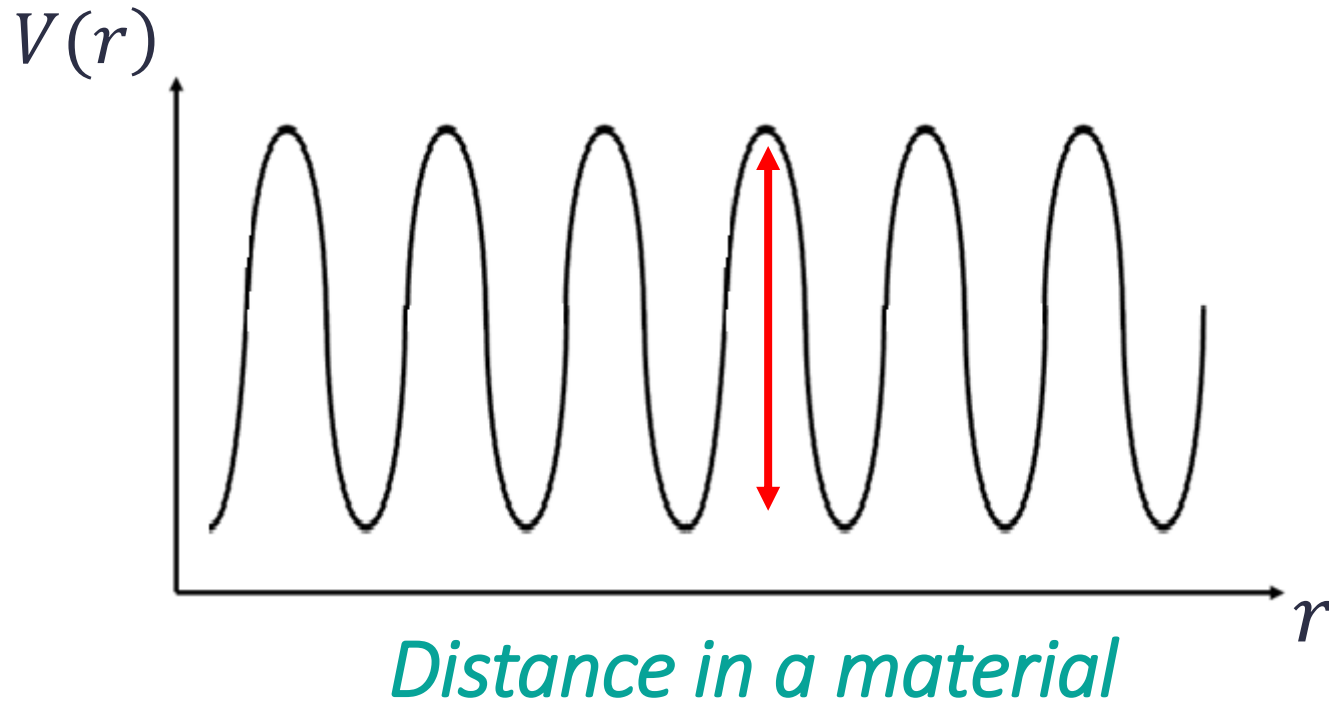
Potential energy as a function of distance in a material

# What does a potential energy of a material look like?

For a periodic system:

$V(r)$

Barriers for charge transport

Minimum energies at electronegative groups

Distance in a material

r

Potential energies of metals vs. insulators?

For an insulator the barriers are high:

Distance in a material

Potential energies of metals vs. insulators?

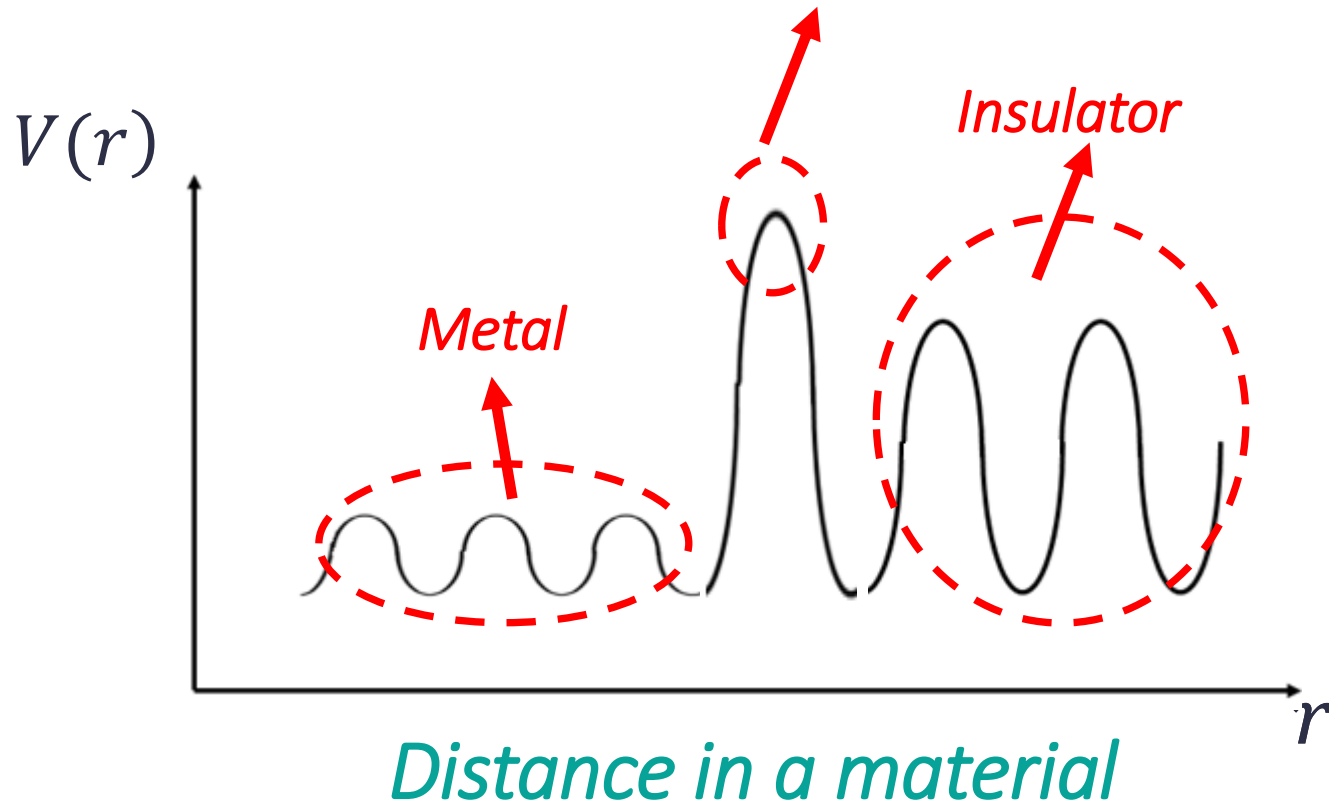For an ideal metal there should be no barriers (charge is free):

$V(r)$

Distance in a material

r
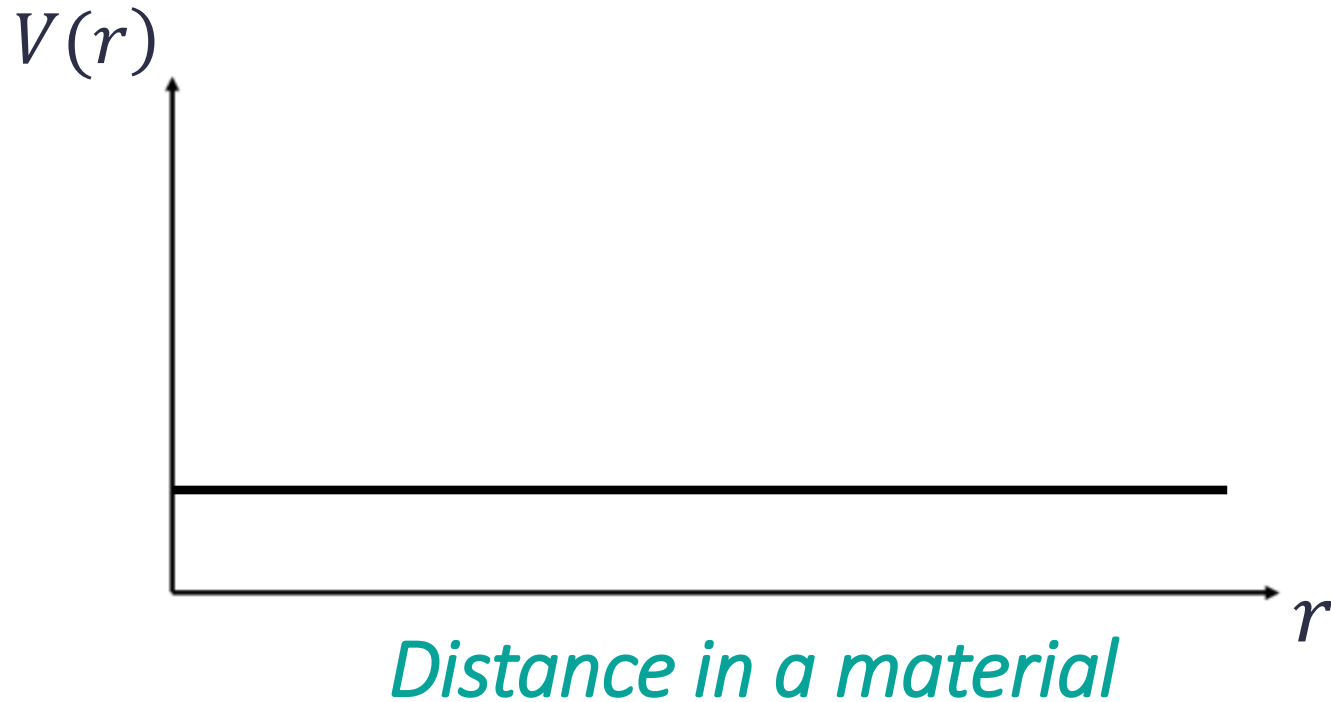
Potential energies of metals vs. insulators?

But there are some low barriers in metals:

Distance in a material
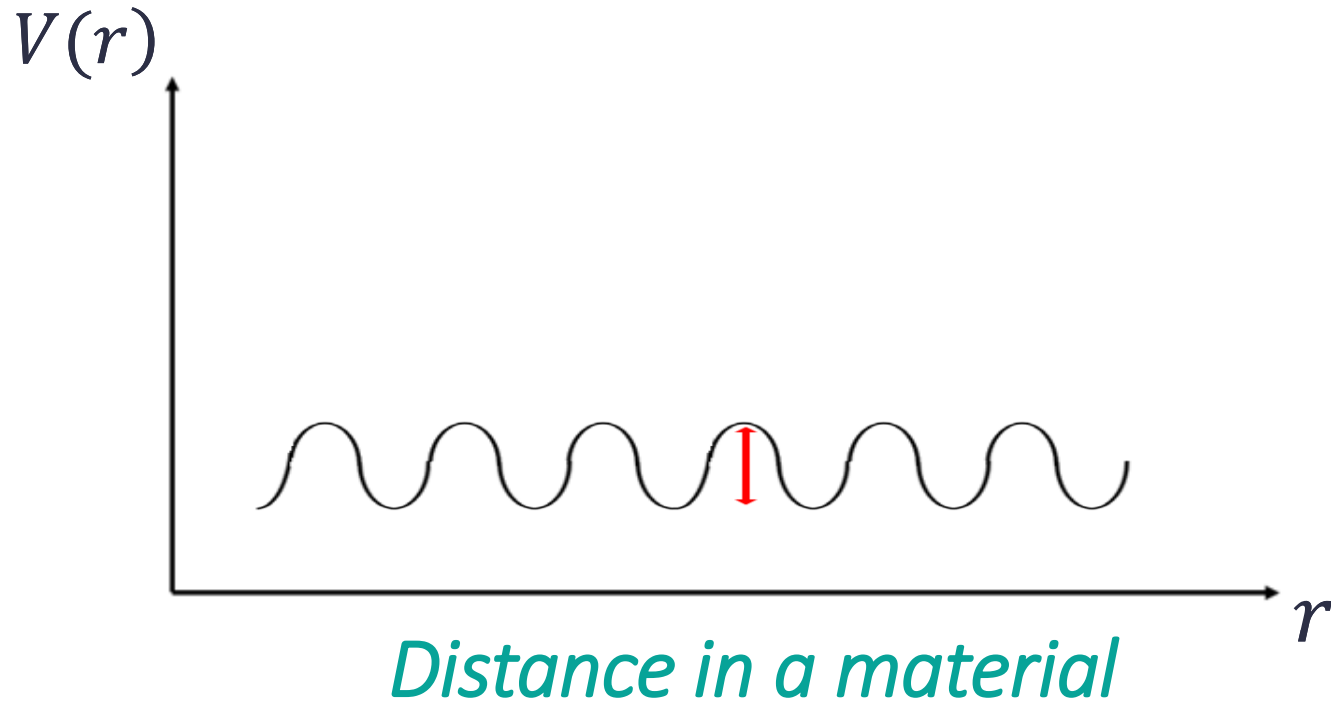
Potential energies of interfaces

New chemical bonds and barriers at the interface:

Interfaces are important for material design.

Step 1: **Characterizing several metal/oxide interfaces**

Ag/Fe2O3
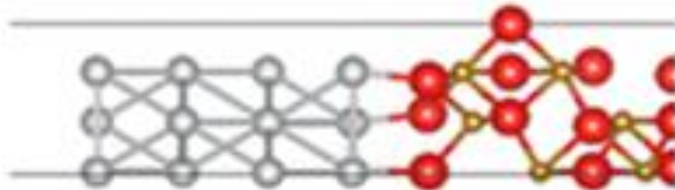
Au/Fe2O3
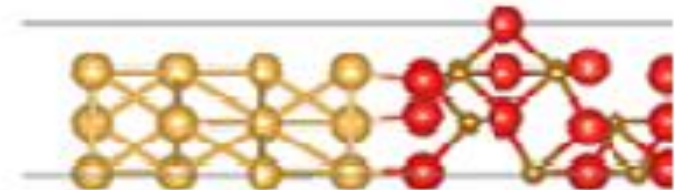
Legend:
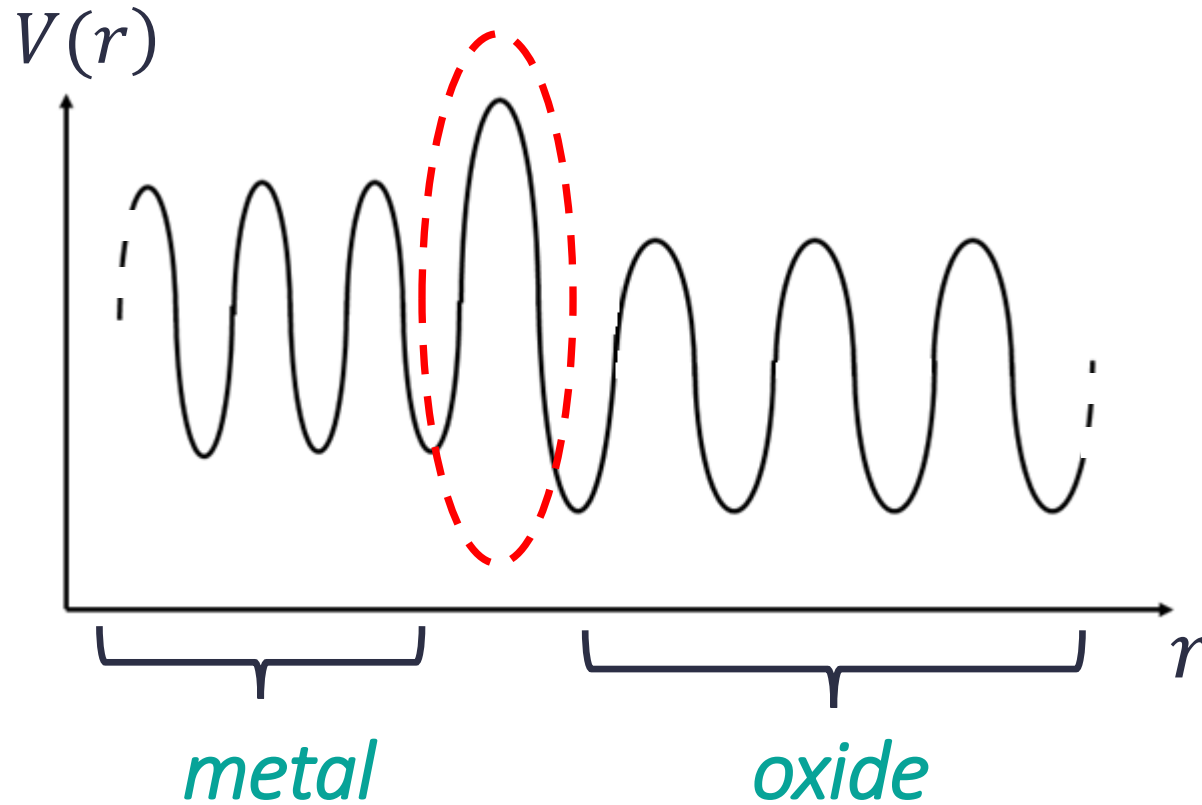- ○ Ag
- ● Au
- ● Oxygen
- ● Fe

$$\hat{H}\left|\psi\right\rangle = E\left|\psi\right\rangle$$

Density Functional Theory (DFT)

$$\psi(\vec{r}_1, \vec{r}_2, ..., \vec{r}_N) \rightarrow \rho(\vec{r})$$

42

Step 2: **A numerical model**

$$\hat{H}\left|\psi\right\rangle = i\hbar\frac{d\left|\psi\right\rangle}{dt}$$
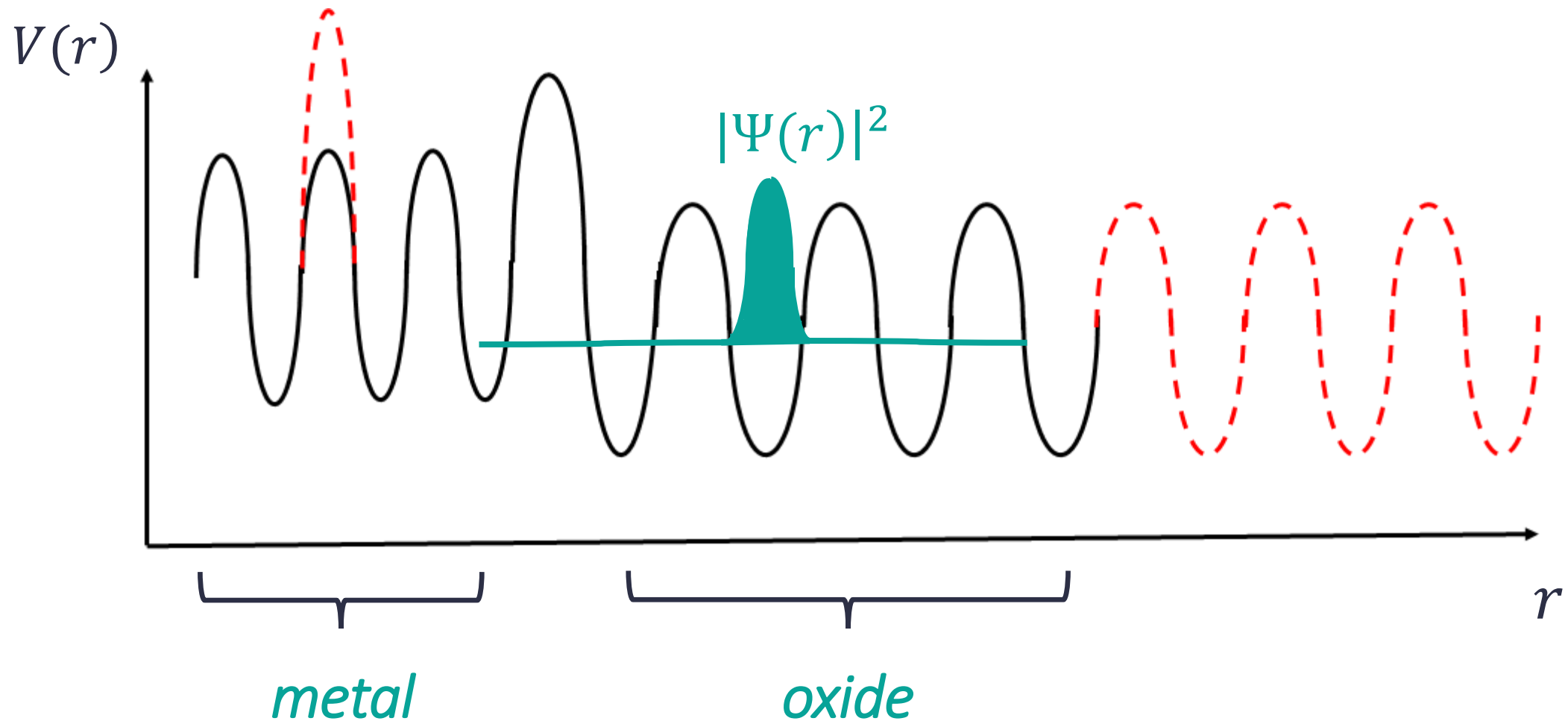
Generalizing the problem to material potentials that change with time at time scales that are important for charge transport at steady state.

$$\hat{H} = \hat{T} + \hat{V}(t)$$
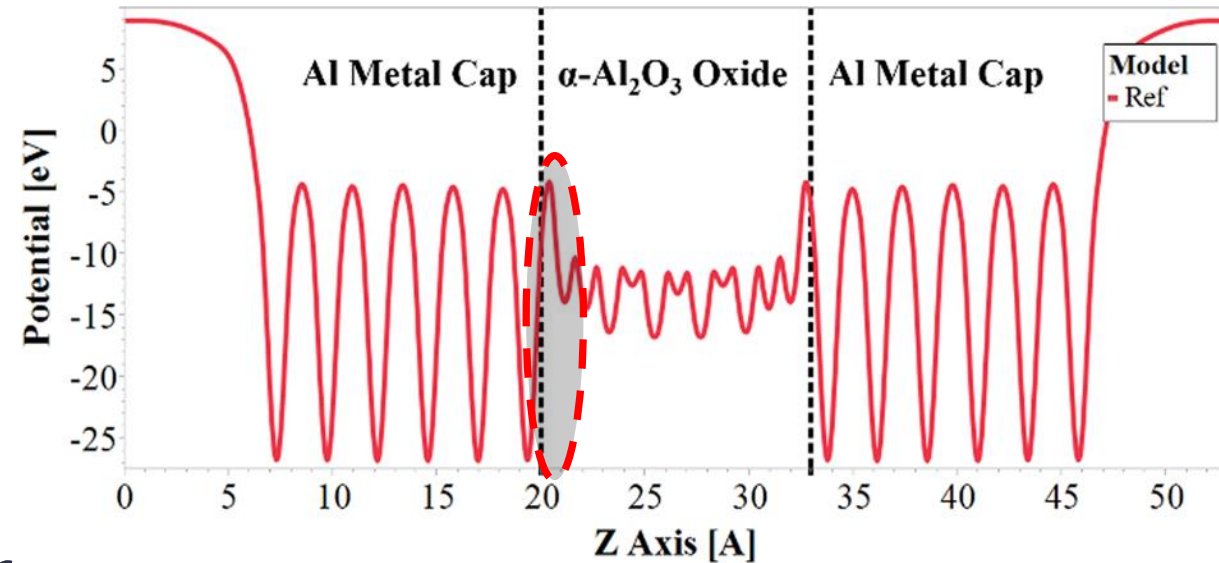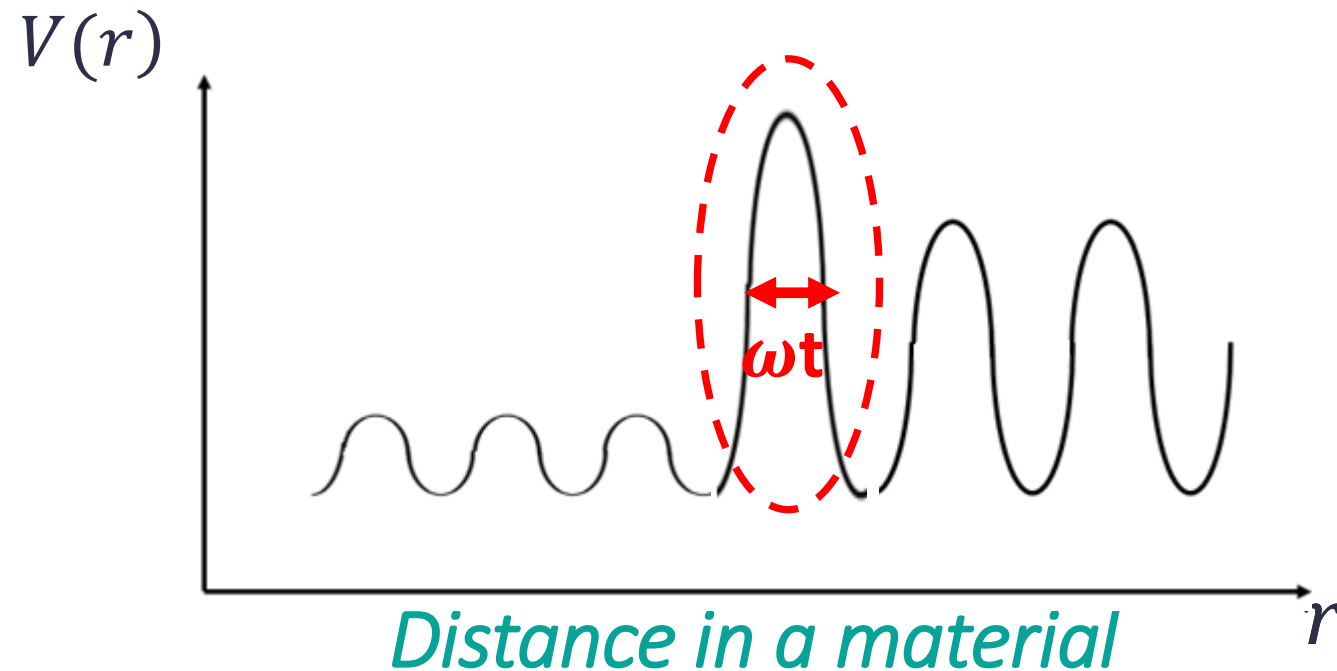
A. Reshef and M. Caspary Toroker, NPJ Comp. Materials 7, 165 (2021).

Larger barrier for a Al vacancy in the oxide:
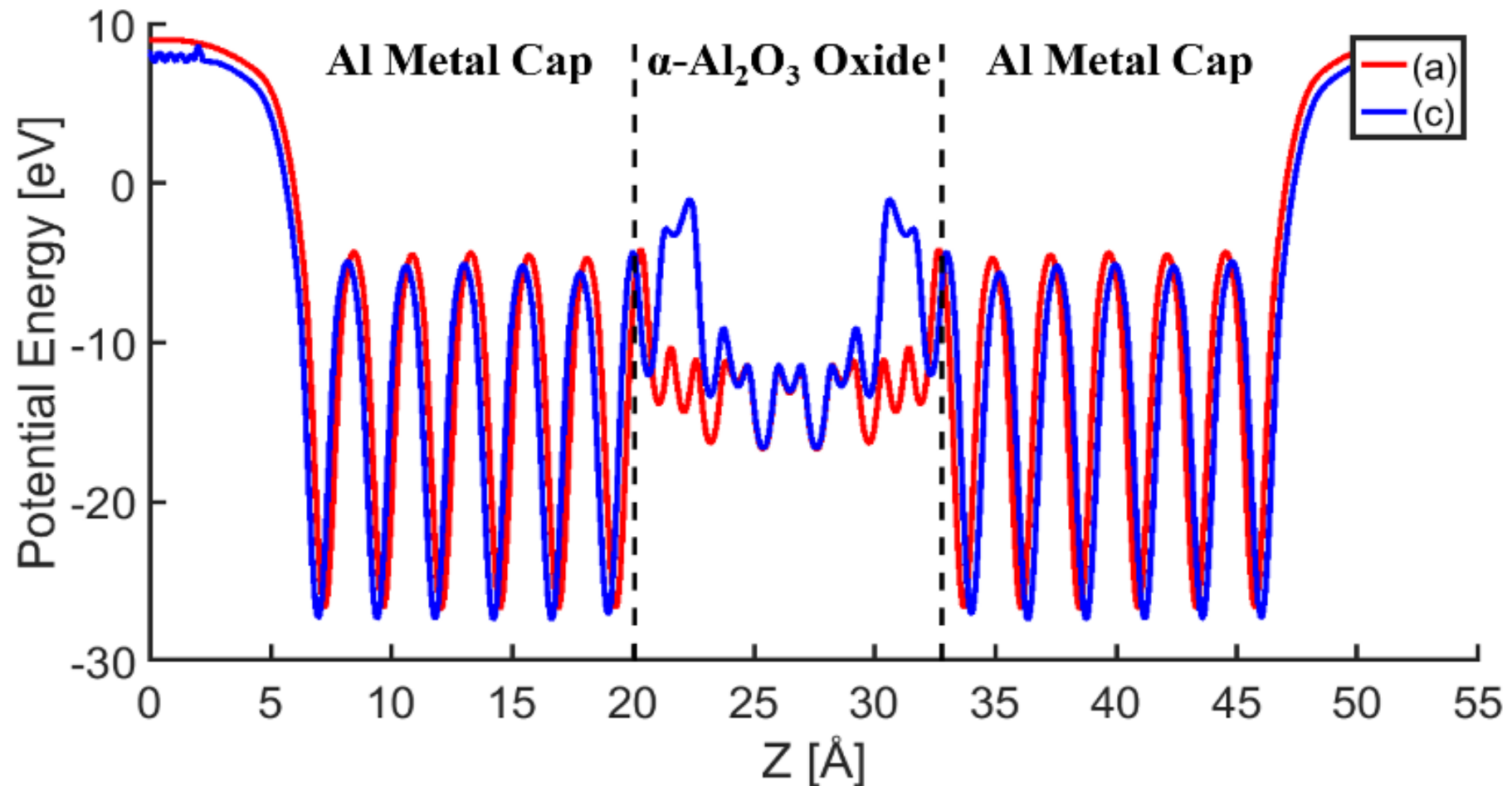
A. Reshef and M. Caspary Toroker, NPJ Computational Materials 7, 1 (2021).

Potential energy for dielectric materials

Mo ●   S ●   C ●   Si ●

$V(r)$

$|\Psi(r)|^2$

V_{eff} [eV]

ϕ_{gap}

ϕ_{TB}

ϕ_{MoS2}

ϕ_{mat}

distance [Ang] along [001]
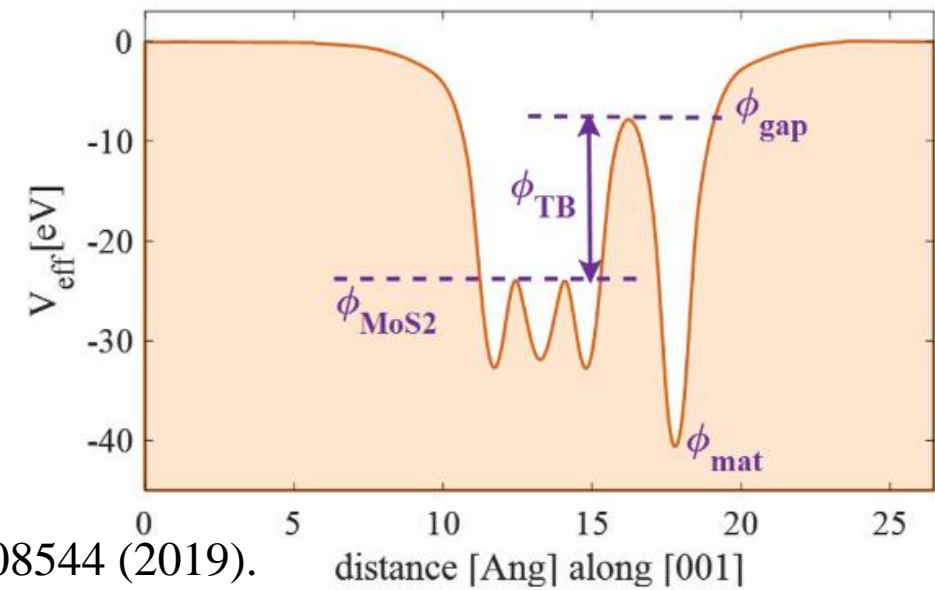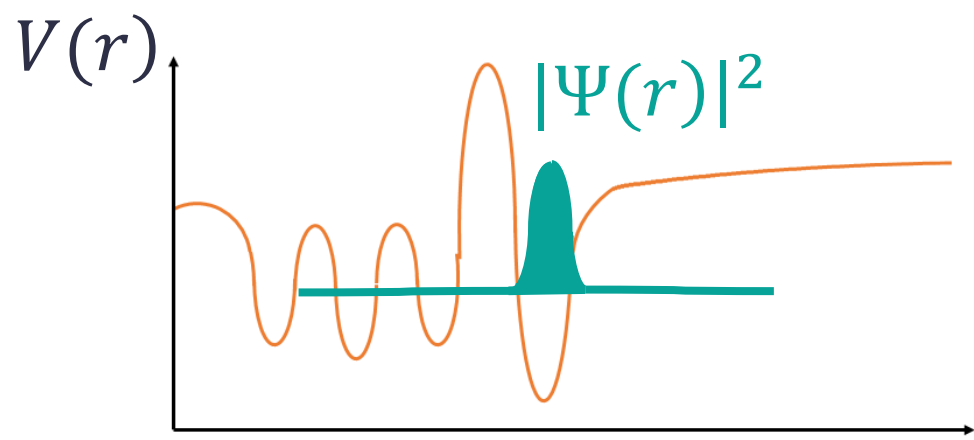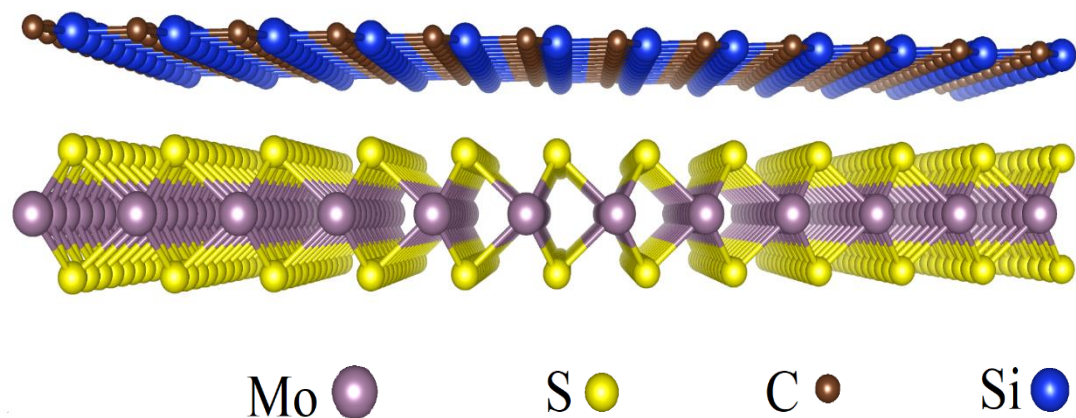
L. Teitz and M. Caspary Toroker, Adv. Func. Mat., 1808544 (2019).

Potential energy for metal/oxide interfaces

Ag ○ Fe ○ Au ○ O ●

$V(r)$

$|\Psi(r)|^2$

Potential [eV]

$Z - axis$ [Å]
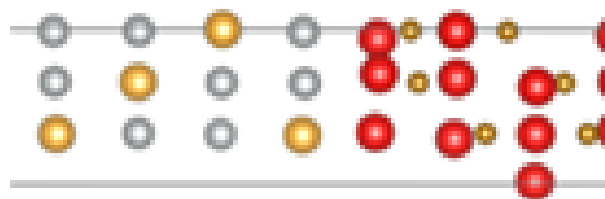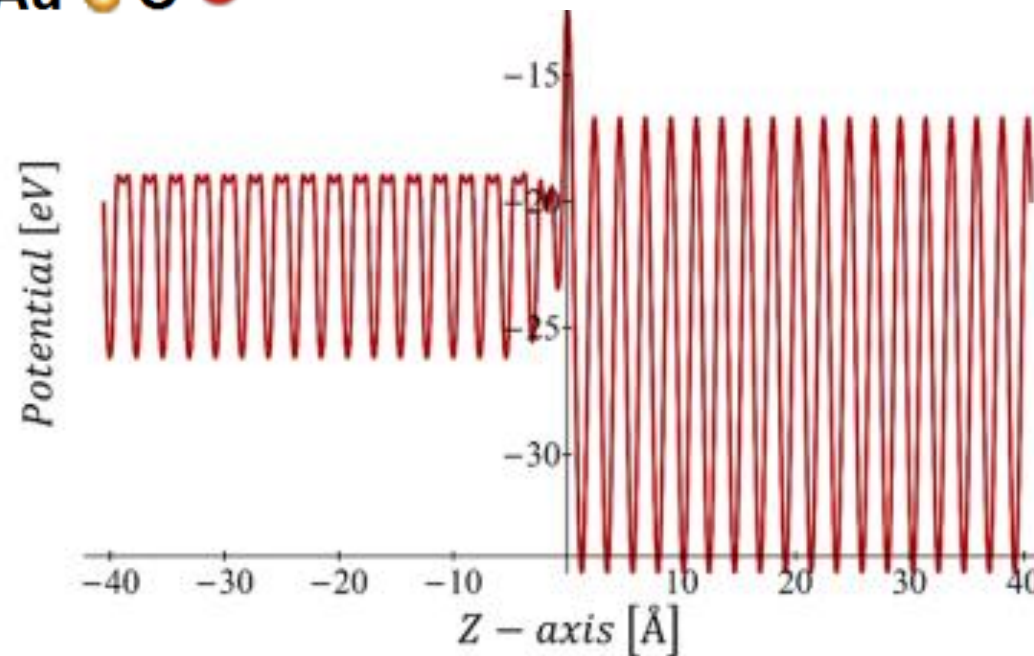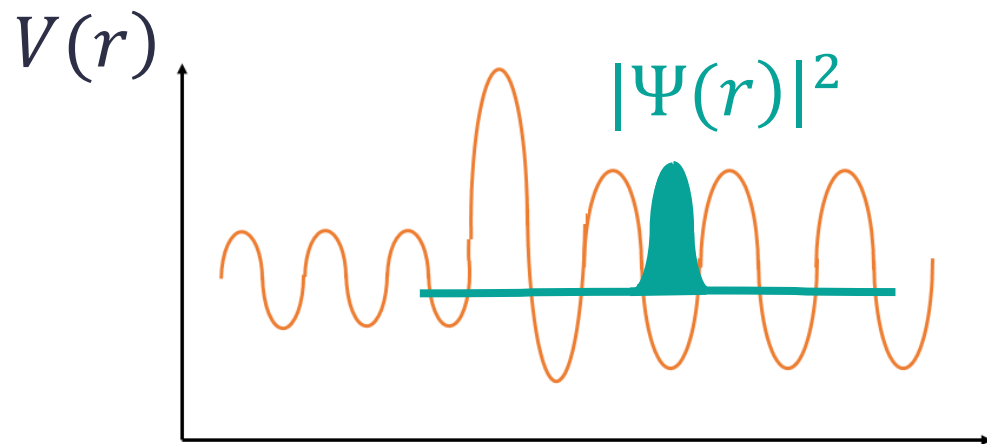
O. Neufeld and M. Caspary Toroker, J. Chem. Theo. Comp. 12, 1572 (2016).

Potential energy in 2D space

$$V = \begin{bmatrix} V(z_1,x_1) & \cdots & V(z_N,x_1) \\ \vdots & \ddots & \vdots \\ V(z_1,x_M) & \cdots & V(z_N,x_M) \end{bmatrix},$$
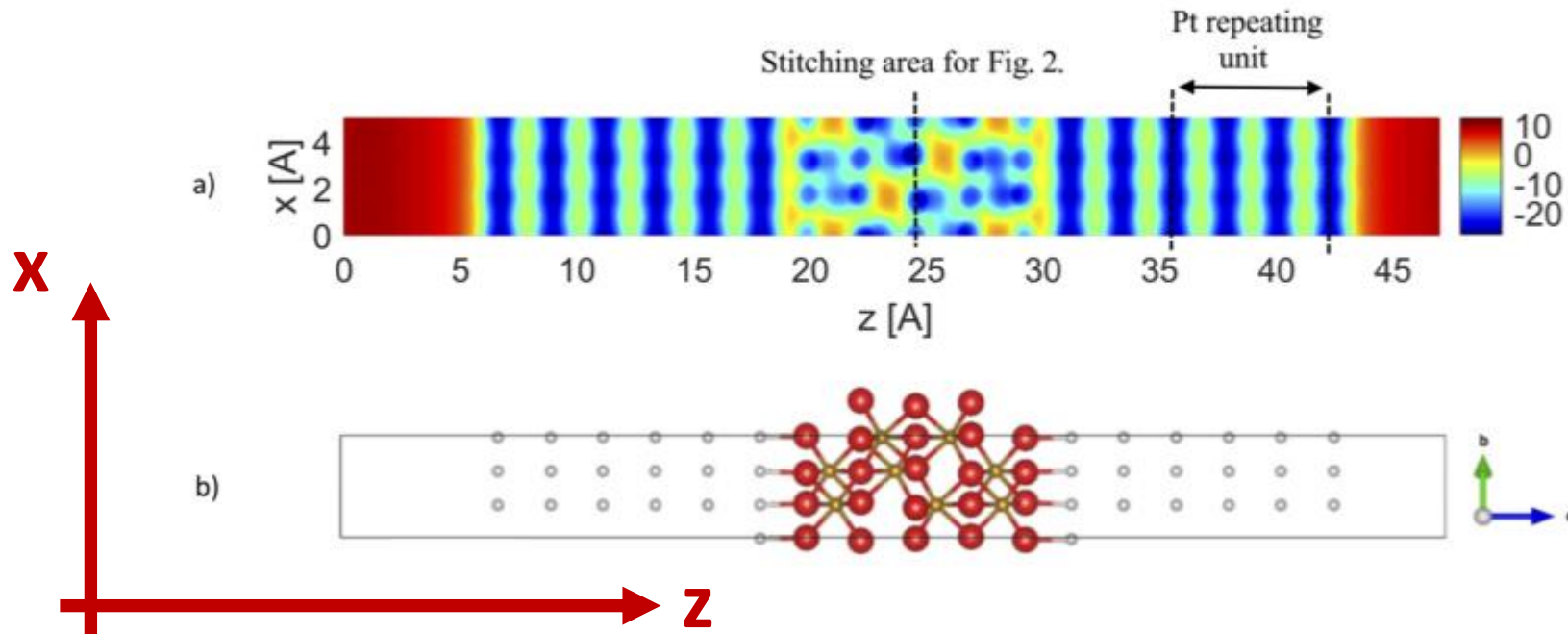
FIG. 1. (a) DFT-calculated Pt/Fe$_2$O$_3$ interface potential matrix. Left and right edges are the vacuum potential. The Pt repeating unit and oxide expansion stitching area are marked. The color bar is given in [eV]. (b) Atomic structure of the interface. Red—O, yellow—Fe, and silver—Pt.

An algorithm to predict transmission through alloys
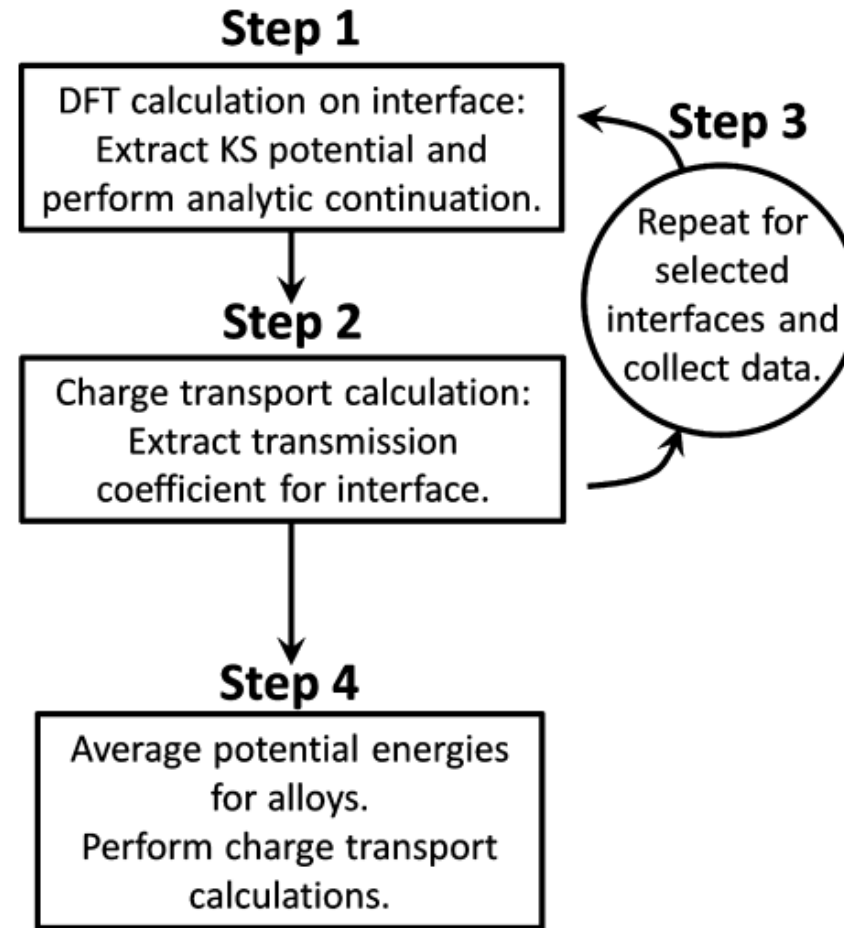
Figure 1. Scheme of the novel high-throughput screening approach for metal/oxide interfaces.

O. Neufeld and M. Caspary Toroker, J. Chem. Theo. Comp. 12, 1572 (2016).

Correlations for material design
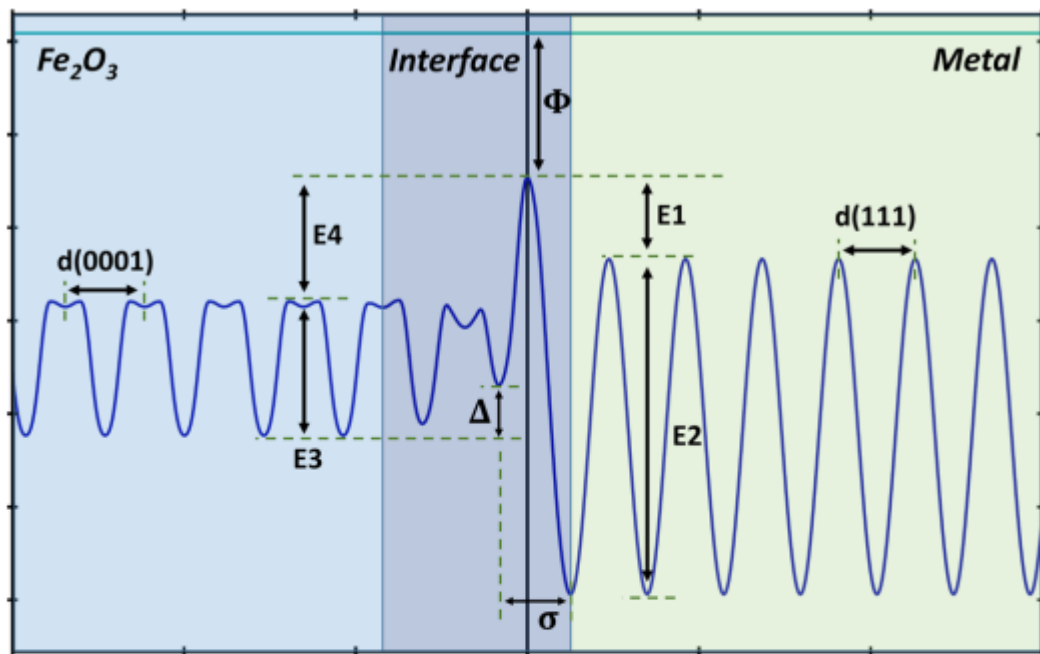
Figure 5. A typical Fe_2O_3/Mt potential energy function and characteristic model parameters: d(111) is metallic (111) planar spacing, E1 and E2 are potential energy levels in the metal, E3 and E4 are potential energy levels in the oxide, d(0001) is the oxide's (0001) planar spacing, Φ is the wave packet's excess energy with respect to the interface barrier, Δ is the potential energy bending in the oxide, and σ is the barrier width. Light blue, blue, and green areas represent bulk Fe_2O_3, interface, and bulk metal regions, respectively.
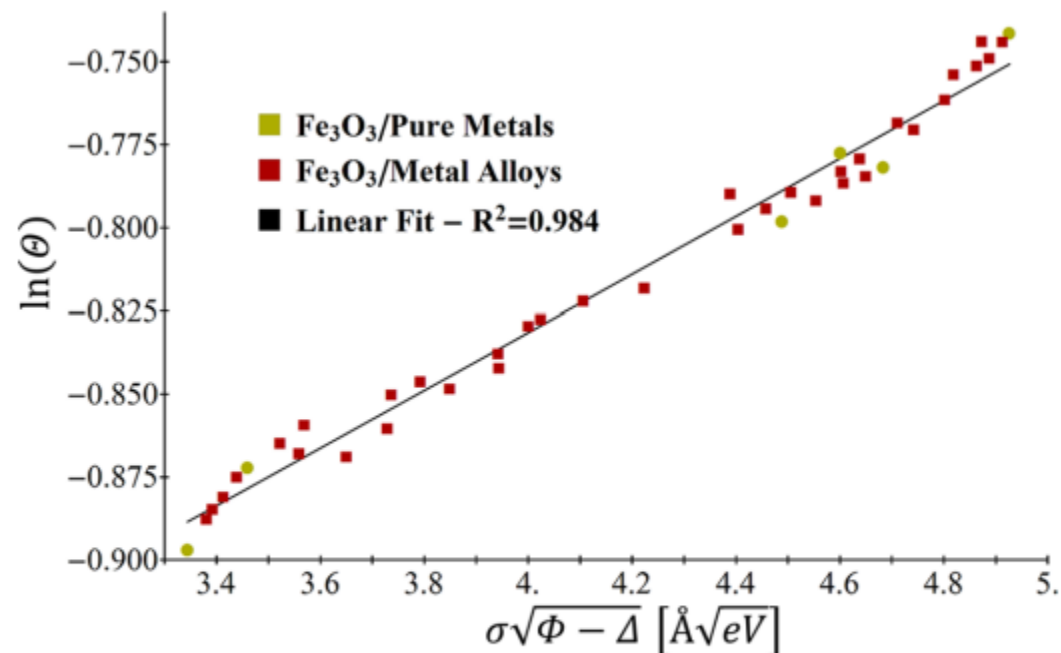
Figure 9. Fe_2O_3/Mt interface data points for $\ln(\Theta)$ as a function of $\sigma\sqrt{\Phi - \Delta}$ against least-squares fit of eq 9.

O. Neufeld and M. Caspary Toroker, J. Chem. Theo. Comp. 12, 1572 (2016).

Codes from our group: importing potential

Mathematica
(Ofer thesis)

```
path = "D:\\.....\\LOCPOT"; (*path to LOCPOT file*)

str = OpenRead[path]; (*open path*)

system = Read[str, String]; (*start reading in lines from LOCPOT file*)
```

Matlab
(Liora thesis)

```
%this function subtracts the non-zero value of the vacuum energy from
VASP's local potential and returns the new potential, the special grid and
the value of the vacuum energy
function [f,g,h] = InputPotential(filename, sheet, zrange, potrange)
z = xlsread(filename, sheet, zrange); %angstrom
z = z*10^-10; % angstrom to m
v0 = xlsread(filename, sheet, potrange); %eV
VacEnergy = max(v0); %eV
v0 = (v0 - VacEnergy)*1.6*10^-19; %subtracting vacuum energy, eV to J
f = v0;
g = z;
h = VacEnergy;
end
```

Same potential used for work function calculations.

The charge starts as a wavepacket with an initial location and momentum:

$$\psi_0(z) = \frac{1}{\pi^{1/4}\sigma_0^{1/2}} \exp\left[\frac{-(z-z_0)^2}{2\sigma_0^2} + i\frac{p_0 z}{\hbar}\right]$$

Initial momentum is extracted from:

$$E_c = \left\langle \psi_0 \mid \hat{H} \mid \psi_0 \right\rangle = \left\langle \psi_0 \mid \hat{T} + \hat{V} \mid \psi_0 \right\rangle = \overbrace{\left\langle \psi_0 \mid \hat{T} \mid \psi_0 \right\rangle}^{T_0} + \overbrace{\left\langle \psi_0 \mid \hat{V} \mid \psi_0 \right\rangle}^{V_0}$$

$$
\begin{aligned}
T_0 =\ & \frac{\hbar^2}{2m}\left(k0^2 + \frac{1}{\Delta x^2}\right) \\[6pt]
& + \frac{i\hbar^2 k0}{2mA}\left\{\exp\left(-\left(\frac{x0}{\Delta x}\right)^2\right) - \exp\left(-\left(\frac{L-x0}{\Delta x}\right)^2\right)\right\} \\[6pt]
& - \frac{\hbar^2}{4mA\,\Delta x}\left[\frac{\sqrt{\pi}}{2}erf\left(\frac{L-x0}{\Delta x}\right) - \left(\frac{L-x0}{\Delta x}\right)\right. \\[6pt]
& \times \exp\left(-\left(\frac{L-x0}{\Delta x}\right)^2\right) - \frac{\sqrt{\pi}}{2}erf\left(\frac{-x0}{\Delta x}\right) + \left(\frac{-x0}{\Delta x}\right) \\[6pt]
& \times \left.\exp\left(-\left(\frac{x0}{\Delta x}\right)^2\right)\right]\Big\}
\end{aligned}
$$

(7)

Codes for the initial wavefunction

Mathematica
(Ofer thesis)

$$\Psi 0\,[x\_]\;:=\;N\left[\frac{\sqrt{\beta}}{\pi^{1/4}}\;\mathrm{Exp}\left[\frac{-\beta^2}{2}\,(x-x0)^2+I\,\frac{p0\,x}{(eV2J\,10^{20})\,\hbar}\right]\right];$$

$$V0\,[x0\_,\;\sigma\_,\;L\_]\;:=\;\mathrm{NIntegrate}\left[\frac{e^{-\frac{(x-x0)^2}{\sigma^2}}}{\sqrt{}}\,V[x],\;\{x,\;-L/2,\;L/2\}\right]\;//\;\mathrm{Re};$$

$$p0\;=\;\mathrm{Max}[(P0\;/.\;\mathrm{NSolve}[(Et+Efermi)\;==\;V0[x0,\;\sigma,\;L]+T0[me,\;\sigma,\;L,\;x0,\;\hbar,\;P0],\;P0])];$$

Matlab
(Liora thesis)

```
psi = exp(-((x-(x0)).^2)/(2*((sqrt(2)*sigma(1))^2)));

V0 = d*trapz(func);

T0 =
const*(sqrt(pi)*sigma(1)*(1+2*(sigma(1)^2)*(kstart^2))*(erf(x0/sigma(1))+er
f((L-x0)/sigma(1))) + 2*(x0+2*1i*kstart*(sigma(1)^2))*exp(-
(x0^2)/(sigma(1)^2)) + 2*(L-x0-2*1i*kstart*(sigma(1)^2))*exp(-((L-
x0)^2/(sigma(1)^2)));
k0 = (double(solve(T0+V0 == E0, kstart)));
```

Time propagation of the wavefunction

- Using the split-step method:

$$e^{-\frac{i}{\hbar}(\hat{T}+\hat{V})dt}|\psi\rangle \approx e^{-\frac{i}{2\hbar}(\hat{V})dt} e^{-\frac{i}{\hbar}(\hat{T})dt} e^{-\frac{i}{2\hbar}(\hat{V})dt}|\psi\rangle$$

- The operation of the kinetic energy is solved in Fourier space:

$$e^{-\frac{i}{\hbar}(\hat{T})dt}|\psi\rangle = \hat{F}^{-1} e^{-\frac{i\hbar^2 k^2}{2m\hbar}dt} \hat{F}|\psi\rangle$$

Codes for time propagation

Mathematica
(Ofer thesis)

$$\text{fftr} = \text{RotateRight}\left[\text{Fourier}[\psi], \text{Floor}\left[\frac{Nz}{2}\right]\right];$$

$$\psi = \text{InverseFourier}\left[\text{RotateLeft}\left[KX * (\text{fftr}), \text{Floor}\left[\frac{Nz}{2}\right]\right]\right];$$

Matlab
(Liora thesis)

```matlab
% calculating the wave function at t+deltat using the split operator
approximation of the second order

psi = exp(-1i*v.*deltat/(2*hbar)).*psi;

F = fft(psi);
phase = exp(-1i*(k.^2)*(hbar*deltat)./(2*m));
phi = phase.*F;
psi = ifft(phi);

psi = psi.*exp(-1i*v.*deltat/(2*hbar));
```

The flux observable

- The flux at each z location

$$j(z, t) = \frac{i\hbar}{2m}\left(\psi\frac{d\psi^*}{dz} - \psi^*\frac{d\psi}{dz}\right)$$

- The flux at z=0:

$$\hat{F}(t)|\psi\rangle = \frac{i\hbar}{2m}\left(\psi(t, z = 0)\frac{d\psi^*}{dz}\bigg|_{t,z=0} - \psi^*(t, z = 0)\frac{d\psi}{dz}\bigg|_{t,z=0}\right)|\psi\rangle$$

$$\equiv F(t)|\psi\rangle \qquad\qquad\qquad (7)$$

- The total probability for charge transport:

$$\Delta Q_{t_0 \to t_f} \equiv \Delta Q(t_f) = \int_{t_0}^{t_f} F(t)dt \approx \sum_{i=1}^{N_t} \frac{F(t_{i+1}) + F(t_i)}{2}\Delta t$$

Codes for flux calculation

Mathematica
(Ofer thesis)

$$J[[iter, \ ;;]] = \frac{\hbar}{me} \left(eV2J \ 10^{20}\right) Im\left[\left(Conjugate[\psi] * InverseFourier\left[\right.\right.\right.$$

$$RotateLeft\left[(-I \ k) * RotateRight\left[Fourier[\psi], Floor\left[\frac{Nz}{2}\right]\right], Floor\left[\frac{Nz}{2}\right]\right]\right]\right];$$

$$ChargePass = Table\left[Trapezoid[J[[1 \ ;; \ n, \ int]]] * \frac{dt}{\Delta R}, \{n, 1, iter - 1, 1\}\right];$$

Matlab
(Liora thesis)

```
%calculating the probability current [e/(A^2*sec)]:

G1 = 1i*k.*F;
dlpsi = ifft(G1);
J = [ J , (hbar/m)*imag(conj(psi(xint)).*dlpsi(xint))];
P = [ P , deltat*sum(J)];
```

Summary of outline #2:

- The **shape of the potential energy** for a material depends on periodicity and chemical composition.
- The potential offers diagnostics based on barrier **heights/widths and code development: dimensionality, time dependence, alloy algorithm.**
- The code is simple and **short**. Anyone can code or use it.

Summary:

- Charge transport through materials is important for a variety of fields, including **electrocatalysis**.
- **Viewing the potential energy of materials** is instructive for understanding potential barriers limiting charge transport.
- We suggest **a new method** for calculating charge transport across materials by obtaining the potential energy from DFT that is **accessible to everyone**.
- There are many **advantages and potential** for the new method, mostly flexibility and control over the potential energy.
- Several **developments** of the code and **applications** to a wide range of materials were demonstrated.

Acknowledgements

Funding:

Group members:

Undergraduate students: Yanai, Sofia, Maya, Efrat, Sigal.
Previous members: Gabi, Liora, Almog.
Current members working on the code: Nadav, Yair.

Thank you for the attention